STATIC AND DYNAMIC ANALYSIS OF GEOGRID REINFORCED UNPAVED ROAD

A Thesis Submitted in Partial Fulfilment of the Requirements for the

Degree of Master of Technology (Research)

In

Civil Engineering

(Geotechnical engineering)

Submitted By

SUJATA PRIYADARSHINI

(Roll Number: 612CE1007)

Under the guidance and supervision of

Dr. S.K.Das

and

Prof. G.L.Sivakumar Babu(IISc,Bangalore)

DEPARTMENT OF CIVIL ENGINEERING

NATIONAL INSTITUTE OF TECHNOLOGY, ROURKELA

2015

National Institute of Technology

Rourkela

CERTIFICATE

This is to certify that the thesis entitled **"Static and Dynamic Analysis Of Geogrid Reinforced Unpaved Road''** being submitted by Sujata Priyadarshini in partial fulfillment of the requirements for the award of Master of Technology (Research) Degree in Civil Engineering with specialization in GEOTECHNICAL ENGINEERING at National Institute of Technology Rourkela, is an authentic work carried out by her under our guidance and supervision. To the best of my knowledge, the matter embodied in this report has not been submitted to any other university/institute for the award of any degree or diploma.

Dr. SARAT K. DAS
Department of Civil Engineering
National Institute of Technology
Rourkela

Prof. G.L. Sivakumar Babu
Department of Civil Engineering
Indian Institute of Science
Bangalore

Place:

Date:

ACKNOWLEDGEMENTS

The work reported in this thesis was carried out under the esteemed supervision and guidance of **Prof.G.L.Sivakumar Babu** and **Prof.S.K.Das.** Foremost, I wish to express my deep sense of gratitude for my supervisor who always supported my endeavours all the time. His continuous guidance was not only helpful in learning the basics of my research work, but also played a vital role in the overall development of my personality. I would like to endow my hearty regards to him for sharing his research experiences and letting me experience the research facilities at IISC and in the field, the practical issues beyond textbooks. There have been numerous occasions where I was never up to the mark, needless to say their patience in understanding and supporting me during those times cannot be forgotten.

I extend my sincere thanks to the Head of the civil engineering Department Prof. S.K.Sahoo for his support over the year. I would like to take this opportunity to thank my Parents and my husband for their unconditional love, moral support and encouragement for the completion of this .

I am grateful for the affectionate forbearance and continuous encouragement and support received from my. Friends who has been a great support throughout the course of research.

I am finally grateful to the Indian Institute of Science (IISC) for providing all the facilities, pleasant ambiance and work culture for successful completion of this work.

Sujata Priyadarshini

Roll no-612ce1007

Date: **Geotechnical Engineering**

ABSTRACT

With Emphasis on greater connectivity, there is a need of unpaved road to achieve economy. In this study a large scale laboratory plate load test was conducted on a circular footing resting on with and without geogrid reinforced bed. Sand and granular materials are used as subgrade and subbase layer. The experiments were conducted for both static and dynamic loading .Test result reveals that with the addition of geogrid the settlement has reduced up to 40-60% as compared to unreinforced section. The experimental static results have validated with numerical modelling using both Finite element method and Finite difference method (Plaxis^{2D} and FLAC^{2D}) and dynamic results have validated by using empirically by Giroud and Han's equation. Based on the experimental and numerical studies, predictive models are proposed using two recently developed artificial intelligent techniques, Genetic Programming (GP) and Multiple adoptive Regression Spline (MARS).

Keywords: Unpaved Road, Geogrid, Reinforcement, Subgrade, Subbase, Dynamic loading, Plaxis^{2D}, FLAC^{2D}, Genetic Programming, and Multiple adoptive Regression Spline

INDEX

Page No

ABSTRACT **i**

LIST OF FIGURE **v**

LIST OF TABLES **vii**

Chapter 1 INTRODUCTION

1.1 Introduction **1**

1.2 Objective and scope of the project **3**

1.3 Organisation of thesis **3**

Chapter 2 LITERATURE REVIEW

2.1 Introduction **5**

2.2 Experimental study **5**

2.3 Numerical Study **8**

2.4 Statistical Study in geotechnical engineering **10**

Chapter 3 EXPERIMENTAL INVESTIGATION

3.1 Materials used **13**

3.1.1 Sand and granular sub base **13**

3.1.2 Geogrid **15**

3.2 Preparation Sand bed and GSB bed **15**

3.3 Experimental setup **16**

3.4 Testing procedure **17**

3.5 Experimental programme **18**

3.6 Result and discussion **19**

3.6.1 Static case **19**

3.7 Strain behaviour of Geogrid **21**

3.8 Dynamic case **23**

3.8.1 Analysis of result and discussion **23**

Chapter 4 Numerical and Analytical study

4.1 Numerical Methods **26**

4.1.1 Introduction to Plaxis^{2D} **26**

4.1.2 Finite Element Modelling (FEM) procedures **27**

4.1.3 FLAC^{2D} (Fast Lagrangian Analysis of Continua) **28**

4.1.4 Finite difference modelling (FDM) procedure **29**

4.1.5 Mohr-Coulomb Material Model **30**

4.1.6 Properties **31**

4.1.7 Result and Analysis **32**

4.2 Evaluation of design methods of geogrid reinforced unpaved roads by J.P. Grioud and Jie Han **35**

4.2.1 Geometry of unpaved structure and Traffic **35**

4.2.2 Axles and loads **36**

4.2.3 Base course material **37**

4.2.4 Bearing capacity mobilization coefficient (m) **37**

4.2.5 Subgrade material **38**

4.2.6 Evaluation of wheel load in pavement **39**

4.2.7 Result Analysis **42**

Chapter 5 Development Of Prediction Models Using Artificial Intelligence Techniques

5.1 Genetic programming **43**

5.1.1 Multi Gene Genetic Programming (MGGP) **45**

5.2 Multivariate Adoptive Regression Spline (MARS) **46**

5.2.1 Forward stepwise algorithm **47**

5.2.2 Backward stepwise algorithm **47**

5.3 Development of prediction model for reinforced bed for static load case **48**

5.3.1 Data base and processing **48**

5.4 Prediction model for dynamic case **53**

5.5 Sensitivity Analysis **66**

5.6 Result and Analysis **68**

Chapter 6 General Observation, Conclusion and Scope of Future study **69**

6.1 Summary **69**

6.2 Conclusion **69**

6.3 Scope for future study **71**

REFERENCES **72**

LIST OF FIGURES

Figure No	Titles	Page No
1.1	Flexible Pavement Section	3
3.1	Grain size distribution curve for sand and granular sub base	13
3.2	Linear Variable Differential Transformer(LVTD)	16
3.3	Schematic representation of test setup	17
3.4	Sectional view of geometry test setup	19
3.5(a)	Case A - Load vs. settlement for 200mm GSB depth	20
3.5(b)	Variation of load with footing settlement for different depth of GSB	21
3.6	Applied stress vs strain in reinforcement (centre)	22
3.7	Applied stress vs strain in reinforcement (edge)	22
3.8	Cross section view of the elongated geogrid after the experiment	23
3.9	Loading patter with respect to number of cycles	24
3.10	Number of cycles vs settlement	24
4.1	A typical Mesh Generation for the present study in PLAXIS^{2D}	28
4.2	A typical Mesh Generated for the present study by FLAC^{2D}	29
4.3	Load Settlement curve for 150mm GSB	32
4.4	Load Settlement curve for 200mm GSB	33
4.5	Load settlement curve for 250mmGSB	33
4.6	Load Settlement curve for 300mm GSB	34

4.7	**Vehicle axle and contact area: (a) Geometry of vehicle axle with dual wheels; (b) Tire contact areas; and (c) equivalent contact area used in analysis**	**36**
4.8	**Number of cycle vs settlement**	**42**
5.1	**Comparison of predicted and measured bearing capacity by MARS for training and testing data in Static case**	**52**
5.2	**Comparison of predicted and measured bearing capacity by GP for training and testing data in static case**	**52**
5.3	**Comparison of predicted and measured bearing capacity by MARS for training and testing data in Dynamic case**	**65**
5.4	**Comparison of predicted and measured bearing capacity by GP for training and testing data in Dynamic case**	**65**

LIST OF TABLE

Table No	Titles	Page No
3.1	Index properties of sand	14
3.2	Index properties of GSB	14
3.3	Geogrid parameters	15
3.4	Testing programme details for GSB bed	18
4.1	Input model parameter used in Plaxis^{2D}	31
4.2	Input model parameter used in FLAC^{2D}	31
4.3	Comparison of experimental and numerical method results	34
4.4	Giroud and Han's equation parameters	41
5.1	Training data for prediction of bearing capacity	49
5.2	Testing data for prediction of bearing capacity	50
5.3	Statistical performance of MGGP and MARS model for Static case	53
5.4	Training data for prediction of settlement for dynamic case	54
5.5	Testing data for prediction of settlement for dynamic case	61
5.6	Statistical performance of MGGP and MARS model for Dynamic case	66
5.7	Sensitivity analysis using MGGP and MARS for static case	67
5.8	Sensitivity analysis using MGGP and MARS for Dynamic case	68

CHAPTER 1
INTRODUCTION

1.1 Introduction

The concept of geosynthetic material was first invented by a French architect and engineer Henri Vidal in the 1960s. In 19th century geosynthetics material was introduced in the geotechnical engineering applications. Different type of geosynthetics materials are extensively used in various forms such as geogrid, geotextile, geocell, geomesh, geonet etc. These are used in the pavement design to address the functions of separation, filtration, lateral drainage and reinforcement. To increase the tensile property of the soil, geogrid have been used in the flexible pavement as reinforcement. Several researchers worked on the geosynthetic reinforced pavement system (Giroud and Noiray 1981, Zornberg 2012) and they suggested that, the distress mechanism induced by the traffic and environmental loads can be decreased. Performance of pavement can be improved due to the geosynthetics reinforcement (Giroud and Han 2004, Bueno et al. 2005, Benjamine et al. 2007).

Flexible pavement generally consists of subgrade, subbase, base and surface course, and pavement structures are made to carry the superimposed load such as traffic load and to well distribute the load safely to the subgrade. In the conventional method of flexible road construction, distress may occur in pavement due to the traffic load or climatic condition. Repetition of traffic load will lead to the structural or functional failure. Environmental loads, such as variations in temperature or moisture in the subgrade can cause surface irregularities and structural distress. Also in case of the conventional method more quantity of material used for the construction of roads and not providing the predicted serviceability. It is necessary to decrease the distresses mechanism in layers, optimize the quantity of materials

In the recent years, various researchers have made conclusion in the use of reinforcement in pavement or foundation bed. There are three primary benefits in using the geogrid, (i) reduce the cost of construction, (ii) reduces the thickness of the pavement, (iii) improvement of the life period of pavement. In order to address the primary issue like fatigue crack in flexible pavement, the geogrid reinforcement is usually used in the interface between subgrade and base course layer or base course and top of the footing.

Several researchers have investigated the evaluation of the ultimate and allowable bearing capacities of shallow foundations supported by sand reinforced with multi-layered geogrid (e.g. Patra *et al*. 2004, Khing *et al*.1993, Das and Omar 1994). The experimental study on triangular aperture geogrid for base course over the weak subgrade under cyclic loading has been carried out by Pokharel *et al*. (2013). Several design methods of geogrid-reinforced pavement have been presented based on empirical, analytical or numerical approaches. Empirical design methods and numerical results have been validated with laboratory model test and then it has been implemented in the field conditions for practical application. But unfortunately, design methods do not typically addressed all the variable like geogrid location and stiffness, base course layer thickness, strength/stiffness of subgrade and base course layer. As a part of this process, factors that affect the performance of geogrid reinforced pavement structures should be determined and evaluated. Keeping all these points in view the design of geogrid reinforced pavement under static and repeated loading has been analysed using various approaches in this study. The schematic representation of pavement with reinforcement as used in the present study is shown in Figure.1.1, in which geotextile has been placed in separation of subgrade and subbase layer.

Though, analytical and numerical models used are more accurate, but it is very difficult to model the spatial variability of soil. Hence, still empirical models based on statistical methods are in use in modelling in geotechnical engineering. Recently artificial intelligence

(AI) techniques are being used as alternate statistical methods and are found to more efficient compared to statistical methods (Das 2013).

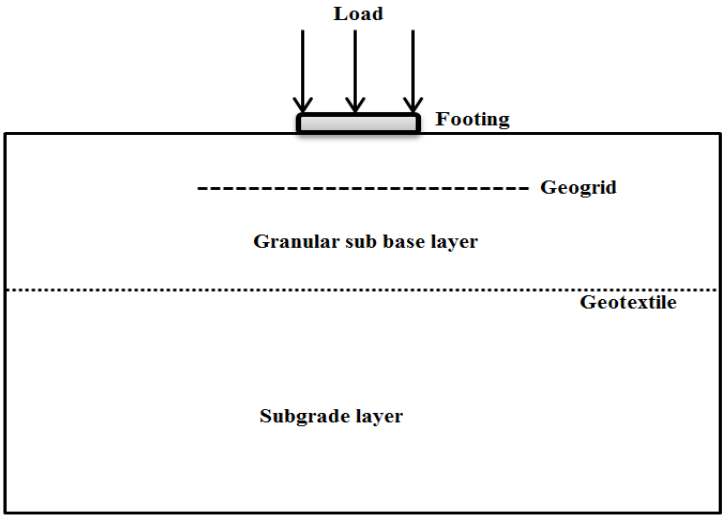

Figure.1.1. Flexible pavement section

1.2 Objective and scope of the project

- Analyses of geogrid reinforced pavement based on model test.
- The result of model study has been validated using numerical methods and analytical methods. Based on the observed results and numerical analysis, a database of settlement and bearing capacity of reinforced pavement is developed, Prediction model equation for bearing capacity and settlement has been presented using the above database using two recently develops AI technique ; genetic programming (GP) and multivariate adaptive regression spline (MARS).

1.3 Organization of the thesis

In Chapter 1, a brief introduction of the present work is presented, with discussion on geogrid and their benefits in pavement. Chapter 2 deals with the literature review of the experimental study, numerical study and analytical methods in geosynthetic reinforced pavement. The

experimental set up used in the present study is discussed in Chapter 3. The materials used for the test and material properties, instruments used in the test, sand bed preparation and procedure to carry out the experiment is also presented in this chapter. Chapter 4 covers the validation of experimental result with numerical and empirical study. Chapter 5 pertains to the results and discussion part of the developed predictive model using GP and MARS and based on the present study the conclusion with scope of future study is included in the Chapter 6.

CHAPTER 2
LITERATURE REVIEW

2.1 Introduction

In the recent years, usage of geosynthetics in the field of civil engineering has been increased rapidly. The combination of soil and geosynthetics usage, finds extensive application in geotechnical engineering constructions.

The following sections summarize the experimental, analytical and numerical studies carried out by various researchers to quantify the effectiveness of geosynthetic reinforcement in pavement construction. Literature on model tests, field experiments and numerical studies is reviewed in separate sections. A brief introduction about the use of artificial intelligence technique for development of prediction model in geotechnical engineering is also presented in this chapter.

2.2 Experimental study

This section discusses about the experimental work carried out by the several researchers in the field of geotechnical engineering to increase stiffness and bearing capacity of the foundation of flexible pavement. It includes a summary of literatures containing the effect of geosynthetics reinforcement in a subgrade layer of flexible pavement and below the footing. The effect of geocell as well as layers of geogrid in highway design, embankment and foundation is also discussed.

DeMerchant *et al.* (2002) conducted an experimental study on geogrid-reinforced lightweight aggregate beds to determine their subgrade modulus. Parameters variability in the study included; soil density (compact and very loose), width of soil reinforcement, location of the top geogrid layer, number of geogrid layers and the tensile strength of geogrid. The results were compared with the data reported in the literature on geogrid-reinforced sand ceramic

beads. It was suggested that, it is desirable to have the width of geogrid reinforcement 4 times the width of a square or diameter of a circular footing. The ultimate bearing capacity obtained from the model test program was compared with the theory proposed by Huang and Menq (1997). For the same soil, geogrid and its configuration and the ultimate bearing capacity and bearing capacity ratio increased with the increase in embedment ratio d_f/B.

Kuo-Hsin Yang *et al.* (2014) worked on the experimental investigations of the behaviour of geogrid reinforced sand featuring reinforcement with anchorages, simulates the reinforcement connected to the wall facings in numerous in-situ situations. Experimental results indicate that relative to unreinforced specimens, both anchored and non-anchored geogrid reinforcements can enhance the peak shear strength and suppress the volumetric dilation of reinforced soil. Geogrid anchorage contributed to a large percentage of the total shear-strength improvement, nearly 3-times more than the contribution of the soil geogrid interaction in non-anchored specimens.

Al-Qadi *et al*. (2008) investigated the geogrid effectiveness in a low-volume flexible pavement. Nine pavement test sections were constructed with base thickness of 203 mm (8in.), 305 mm (12 in.) and 457 mm (18 in.). For this purpose asphalt thicknesses of 76 mm (3 in.) were used, except in one section, where asphalt thickness of 127 mm (5 in.) was used. The pavement test sections were constructed on subgrade with a California Bearing Ratio (CBR) of 4 percent. Based on the accelerated testing results, it was concluded that for a thin base course layer, placing geogrid at the subgrade and base course interface gives better performance and the geogrid should be placed in the upper one third of the base course layer for a thicker base course layer. Henry *et al*. (2009) addressed the potential benefits of geogrid base course reinforcement in flexible pavements. The subgrade material used in their study was silt (ML under Unified soil classification system (USCS) or (A-4 under AASHTO soil classification system). Two asphalt and base thicknesses were used, 102 mm (4 in.) and 152

mm (6 in.) for the asphalt; and 300 (12 in.) and 600 mm (24 in.) for the base course. Each combination of asphalt and base thickness was constructed with and without geogrid. As such, the total of eight test sections has been evaluated. The subgrade has modulus values of approximately 55 MPa (CBR of about 5 percent). Geogrid were placed at the base/subgrade interface for all stabilized sections. The results reported by (Henry *et al*. 2009) showed traffic benefit ratio of 1.3 to 1.4. No benefit was observed in the test section with 600 mm (24 in.) thick base and 150 mm (6 in.) thick asphalt.

Shin *et al*.(1993) conducted laboratory model tests on a surface strip foundation supported by geogrid-reinforced saturated clay to obtain the critical parameters required to derive the maximum ultimate bearing capacity for a given clay-geogrid combination. Similarly, Das and Shin (1994) has also conducted laboratory model tests to determine the permanent settlement of a surface strip foundation supported by geogrid-reinforced saturated clay and subjected to a combination of static and dynamic load of slow-frequency. The result shows that maximum permanent settlement increases with the increase in the intensity of the static load for a given amplitude of the cyclic load intensity. Raymond and Komos (1978) derived the relationship between foundation settlement and the number of load cycles by conducting the model tests on strip surface foundations supported by sand. Das *et al*. (2002) conducted large-scale laboratory model tests to determine the permanent settlement due to cyclic load of the rail road bed for a proposed high-speed train route extending from Seoul to Pusan in South Korea. They evaluated that the permanent settlement of the rail load is constant after the application of 10^5 numbers of cycles and also they concluded that the settlement reduction is reduced more effective when the geogrid placed in between the interface of subgrade and subbase. Tafreshi and Khalaj (2008) performed experimental studies on small-diameter pipes buried in reinforced sand subjected to repeated loads. They concluded that, as the number of

cycle increases the deformation of the pipe and settlement of the soil surface increases respectively.

2.3 Numerical Study

Numerical studies have been carried out by many researchers to calibrate the laboratory and field tests and in-depth investigation of the load transfer mechanism between the reinforcement and soil.

The principle mechanism responsible for reinforcement in paved roadways is generally referred to as a base course lateral restraint. Vehicular loads applied to the road surface create a lateral spreading motion of the base course aggregate. Tensile lateral strains are created in the base below the applied load as the material moves down and out away from the load. The geosynthetic restraints the base, thus reducing the lateral movement. The lateral restraint involves several effects of reinforcement including (i) restraint of lateral movement of base aggregate, (ii) increase in base modulus due to confinement, (iii) improved vertical stress on the subgrade due to increased base modulus and (iv) reducing shearing in the top of subgrade. This study was experimentally verified by Perkins (1999) and lead to reduction in vertical strain in the subgrade and base layer.

Gu (2011) used ABAQUS (ABAQUS UNIFIED FEA SIMULATE REALISTIC PERFORMANCE WITH ADVANCE MULTIPHYSICS SOLUTIONS), Dassault systems, Japan) to model foundation bed and base courses in pavements reinforced with geogrid reinforcement. Soil in the foundation bed was modelled using Drucker-Prager plasticity model, geogrid was modelled using linear elastic truss elements and soil-geogrid interaction was modelled using two contact surface pairs above and below the reinforcement layer. The bearing capacity of reinforced foundation bed increased with an increase in the tensile modulus of the reinforcement and with an increase in the number of layers.

Similarly Nazzal *et al*. (2010) developed a finite-element model with the ABAQUS software package to investigate the effect of placing geosynthetic reinforcement within the base course layer on the response of a flexible pavement structure. Finite element analyses were conducted on different unreinforced and geosynthetic reinforced flexible pavement sections. The results of this study demonstrated the ability of the modified critical state two-surface constitutive model to predict, with good accuracy, the response of the considered base course material at its optimum field conditions when subjected to cyclic as well as static loads. The results of the finite-element analyses showed that the geosynthetic reinforcement reduced the lateral strains within the base course and subgrade layers. The improvement of the geosynthetic layer was found to be more pronounced in the development of the plastic strains rather than the resilient strains. The reinforcement benefits were enhanced as its elastic modulus increased. Also Leng and Gabr (2003) conducted a numerical analysis using ABAQUS to investigate the performance of reinforced unpaved pavement sections. The researchers reported that the performance of the reinforced section was enhanced as the modulus ratio of the aggregate layer to the subgrade decreased. The critical pavement responses were significantly reduced for higher modulus geogrid or better soil/aggregate-geogrid interface property.

Perkins *et al*. (2012) described a two-dimensional finite element model for the simulation of unpaved road test sections. Base aggregate was modelled using a nonlinear elastic model and the reinforcement was modelled as a structural two-node linear elastic membrane element. A contact shear interaction model was used for the interface between the reinforcement and base aggregate. They described a damage (rutting) model for the base aggregate and subgrade layers. Results from laboratory model tests on unpaved road sections were used to calibrate the model.

Palmeira (2009) presented and discussed typical experimental and numerical methods for the study of soil geosynthetic interaction. Emphasis was given to direct shear tests, pull-out tests, in-soil tensile tests and ramp tests. Also Al-Azzawi (2012) carried out finite element simulations of geogrid through ANSYS(engineering simulation software computer-aided significant products of computational fluid dynamics developer headquartered south of Pittsburgh in United States) software and presented the analysis of soil-geogrid interaction to evaluate the benefits of using geogrid in flexible pavements. It was reported that when the geogrid was placed at the bottom of the base course layer, effective bonding was improved between the asphalt concrete and geogrid.

2.4 Statistical study in Geotechnical engineering

The great complexity encountered in Geotechnical engineering such as slope stability, liquefaction, shallow foundation and pile capacity prediction have forced researchers to develop empirical models. Recently various AI techniques are being used as alternate statistical method to develop prediction models in geotechnical engineering and found to be more efficient compare conventional statistical method (Das, 2013). This section presents a brief discussion of AI methods being used in different geotechnical engineering applications.

Artificial Intelligence (AI) techniques such as Artificial Neural Networks (ANNs) and Support Vector Machine (SVM) are considered as alternate statistical methods and are found to be more efficient compared to statistical methods (Das and Basudhar, 2006 and Das *et al*. 2011a). Similar studies have also been made for prediction of lateral load capacity of piles in clay using ANN (Das and Basudhar, 2006). Based on various statistical performance criteria, Das and Basudhar (2006) observed that ANN model is better compared to Broom's and Hansen's method.

Though, the limit equilibrium method is the most widely used methods for the slope stability analysis, statistical methods also have been investigated for the slope stability analysis. Sha *et al*. (1994) initiated the application of statistical method in the prediction of factor of safety in slope stability analysis considering some case studies. Yang *et al*. (2004) proposed a two stepped algorithm of GP and GA to propose a statistical equation for the FOS based on parameters unit weight cohesion (C) and friction angle of soil, height of slope (H), slope angle (ϕ) and pore pressure parameter (r_u). The most important problem associated with efficient implementation of data driven approach is generalization. The model needs to be equally efficient for new data during testing or validation, which is called as generalization. Das and Samui (2007), proposed and investigated with the use of the relevance vector machine (RVM) to determine the liquefaction potential of soil by using actual cone penetration test (CPT) data. RVM is based on a Bayesian formulation of a linear model with an appropriate prior that results in a sparse representation.

Recently Gondami and Alavi (2011, 2012) proposed a variant of GP called Multi Gene Genetic Programming (MGGP) and found to efficient to some test problems in structural geotechnical engineering. Samui *et al*. (2011) observed that the MARS model for uplift capacity of suction caisson has better statistical performance compared to ANN and FEM model. Hence, more research is required in ANN regarding the generalization, control on the model parameters, extrapolation and depicting simplified model equation.

Das and Muduli (2011) analysed the liquefaction potential of soil based on cone penetration test (CPT) data obtained after 1999 Chi-Chi, Taiwan, earthquake using GP, and made a comparative study among the three CPT based statistical methods.

Based on the above discussion it can be seen that various efforts have been made to use geosynthetic/geogrid reinforcement to improve the performance of pavement. Laboratory tests and in-situ investigation shows that there is improvement in terms of stiffness and bearing capacity of pavement with inclusion of geogrid. However, there is need of further laboratory study in this regards with variations in soil layer, reinforcement and its validation through numerical/analytical studies. It was also observed that there is not a comprehensive prediction model for the reinforced pavement.

CHAPTER 3

EXPERIMENTAL INVESTIGATION

Introduction

This chapter discusses the materials properties and result from laboratory model test used in presented study. A discussion about the preparation of the subgrade and granular subbase, experimental setup is discussed. The effect of various parameters studied includes granular subbase depth, strain behaviour of geogrid during static test. The influence of these parameters on the bearing capacity and strain on geogrid is illustrated. The behaviour of the geogrid reinforced granular subbase is explained in terms of strain variation on the geogrid and bearing capacity values.

3.1 Materials used

3.1.1 Sand and granular subbase

In this experiment the sand and gravel are used. The sand was collected and cleaned properly to make suitable as engineering test. The sand is used as subgrade and gravel is used as granular subbase. Grain size distribution curve of sand and gravel are shown in Figure.3.1.

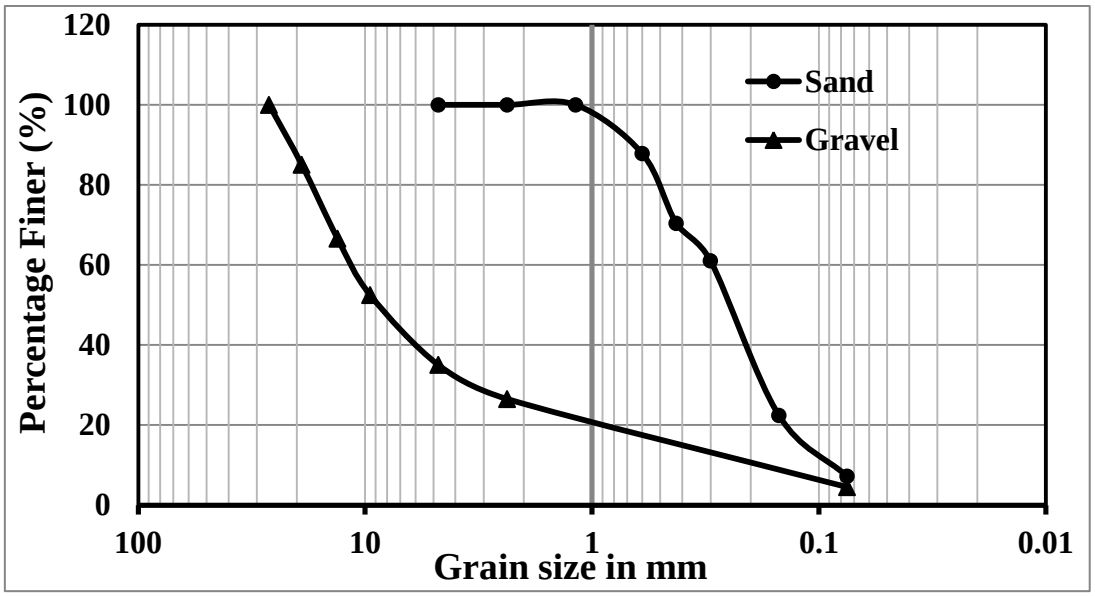

Figure.3.1.Grain size distribution curve for sand and granular subbase.

The other geotechnical properties of the sand and gravel were determined in the laboratory by as per ASTM and Indian standards and their results are presented in Table.3.1 and 3.2, respectively.

Table.3.1. Index parameter of the sand

Parameter	**Value**
D_{10}	0.082
D_{60}	0.30
Coefficient of curvature (C_c)	1.17
Coefficient of uniformity (C_u)	3.66
Maximum dry density of sand(kN/m^3)	20.60
Minimum dry density of sand(kN/m^3)	14.32
Internal Friction angle (ϕ)(Degree)	31

It can be seen that both the sand and gravel are well graded. The granular subbase was placed over the sand using as a base course material to investigate the improvement of load bearing capacity on the pavement. The density of sand was achieved with light compaction mode. The density of GSB was achieved based on a laboratory calibration test.

Table.3.2. Index parameter of the gravel

Parameter	**Value**
D_{10}	0.60
D_{60}	14.00
Coefficient of curvature (C_c)	4.28
Coefficient of uniformity (C_u)	23.33
Mass density of granular sub base (kN/m^3)	17.85
Internal friction angle (ϕ) in degree	42

3.1.2 Geogrid

In the present study biaxial geogrid is using as the reinforcement in granular subbase, having the high tensile strength and stiffness in both direction (MD and XMD). Its parameters are mentioned in the Table.3.3. The main objective for keeping geotextile was separation of granular subbase and sand. Both the reinforcement geotextile and geogrid are simply laid on the tank. They are not fixed at sides of the tank.

Table.3.3. Geogrid parameters

Parameter	Values
Aperture size (MD, XMD)	30mm, 30mm
Ultimate tensile strength (kN/m)	20
Mass per unit area (g/m^2)	200
Shape of the aperture opening	Square

3.2 Preparation of sand bed and granular subbase

In this plate load test, two layer of soil is considered. Sand is used as subgrade material with a depth of 500mm and granular material considered as base course material. The sand bed was laid with a constant density of 20.60 kN/m^3 for all the cases. Granular subbase is laid above the sand bed in equal interval layer of 50mm with predetermined density, after completion of every layer, it is compacted with help of hammer for achieving the required density. The depth of granular subbase varied from 150mm to 300mm from subgrade. A circular model footing having the diameter of 150mm was used. Model footing was placed on the pre-determined alignment at the top surface of the granular subbase. Linear variable differential transformer (LVDT) is used for measuring the settlement of footing during experiment, least count of LVDT is 0.1mm and maximum value 50mm. The granular subbase was prepared by

adding 6% of water with crushed aggregate. The density of the foundation bed was checked by laboratory calibration method.

Figure.3.2 Diagram showing the arrangement of LVTD

3.3 Experimental setup

The experiments were conducted in the test tank of size 1500 mm length x 1500 mm width x 1000 mm height made up of cast iron. The tank was fitted to the loading frame which is connected to the automated load operating system. A circular shaped steel plate with 15 mm thickness and 150 mm diameter was used as the model footing. The bottom of the footing was made rough by coating a thin layer of sand with epoxy glue. The load was applied on the footing through an automatically operating system and load cell was placed in between the footing and actuator to measure the imposed load. Subgrade and granular subbase layer is separated with help of geotextile throughout the experiments. Schematic representation of test setup is shown in Figure.3.3. In the figure loading frame, load cell, actuator, pressure cell and LVDT is shown along with the test bed showing sand bed and GSB bed. In case of pavement with reinforcement, the geogrid reinforcement was placed at a depth of 0.3 times depth of

granular subbase below the footing. The sectional view of the test set up is also shown in Figure 3.4.

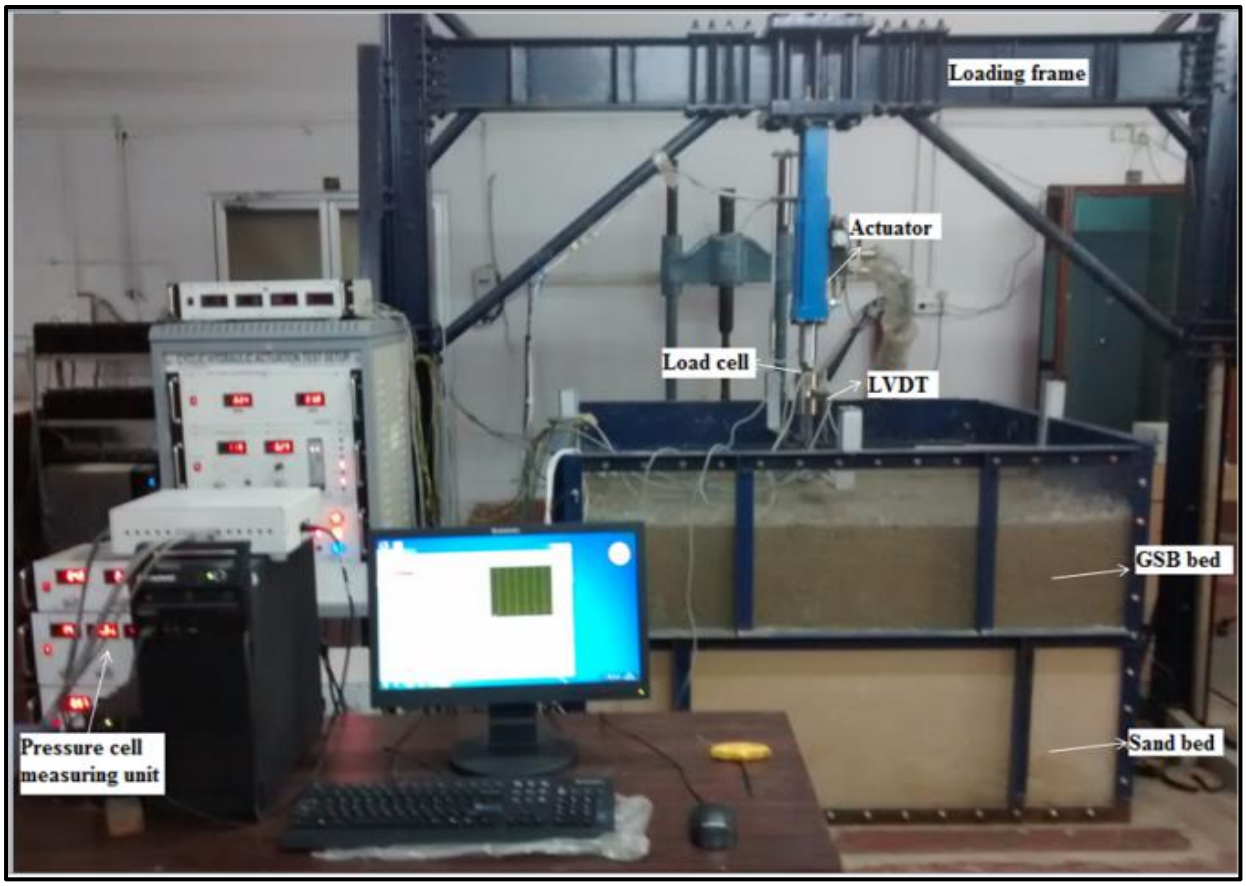

Figure.3.3. Schematic representation of test setup

3.4 Testing procedure

The concentrated vertical load was applied on the footing with the help of ball bearing arrangement. Through the precise measurements, the footing was placed exactly at the centre of the test tank in order to avoid the eccentric loading. The load applied to granular subbase was measured through load cell placed between the footing and the actuator. Four LVDT were placed on the either side of the centreline of the circular footing to record the footing settlement. During experimental study, Static loading tests carried out for all the depths of granular subbase varying from 150mm to 300mm. In case of static loading, load increment was 0.049 kN per second and increased up to 34.33 kN. The magnitude of the load and

settlement were recorded using automatic data acquisition system. A static pressure was first applied to the footing followed by application of the dynamic load. After application of static load immediately the LVTD set to be zero and the dynamic load applied.

3.5 Experimental programme

The details of the testing program are summarized in Table.3.4. The geogrid mesh used was square in shape and width of geogrid (b) is three times the width of footing (B), it was kept constant throughout the experiments. The density of granular subbase, size of footing, relative density of the sand bed, geogrid size and width of geogrid were kept constant in all the tests.

Table.3.4. Testing programme details for granular subbase bed

Test Series	Variable parameters	Constant parameters
A	Type of reinforcement: Unreinforced, geogrid reinforced (granular subbase 200mm)	*b/B*=3, u/d=0.3
B	Unreinforced condition *D*=150mm, 250mm, 300mm	*b/B*=3, u/d=0.3
C	Geogrid reinforced *D*=150mm, 250mm,300mm	*b/B*=3, u/d=0.3

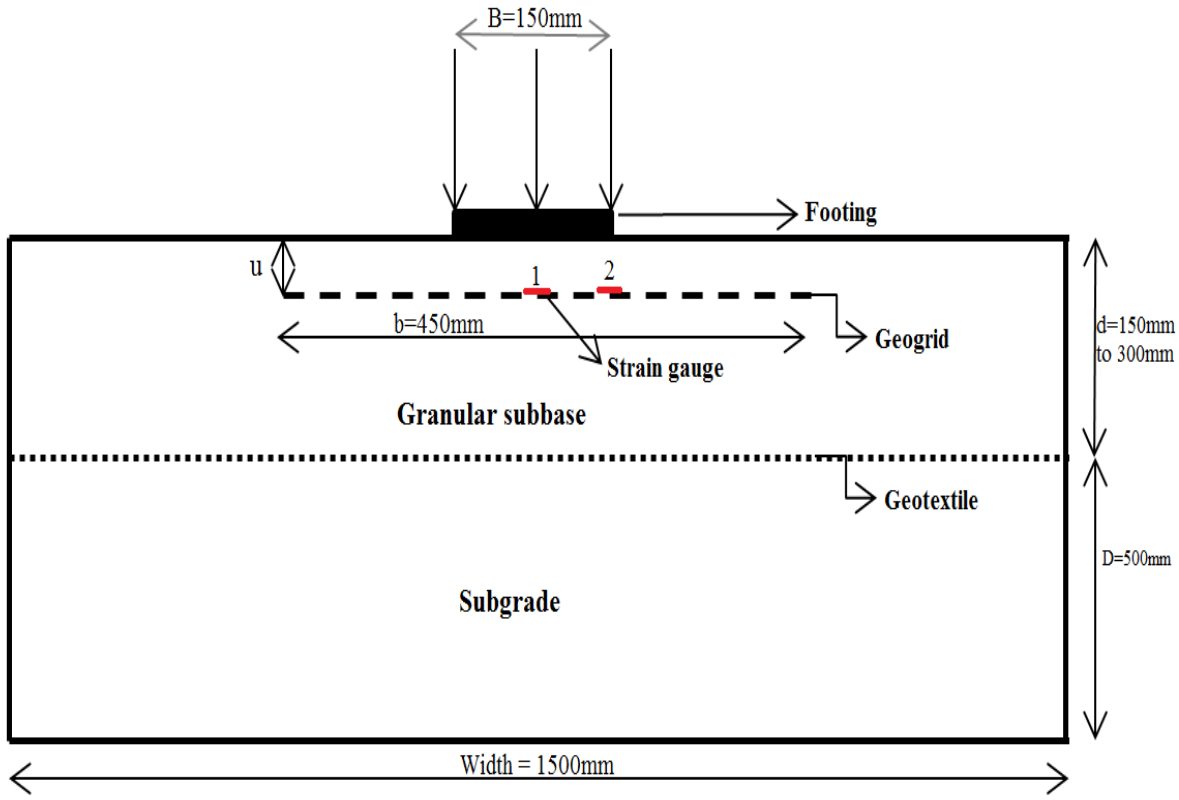

Figure.3.4. Sectional view of geometry test setup

3.6 Results and discussions

3.6.1 Static case

Test series-A was conducted for depth of 200mm granular subbase. Figure.3.5 (a) presents the load and settlement response of the unreinforced and reinforced granular subbase bed. For a particular load at failure, settlement of the foundation bed was observed 20.75mm in case of unreinforced granular subbase and in case of reinforced granular subbase it was observed was 12.55mm. Hence, the settlement is reduced by 40% compared to unreinforced case.

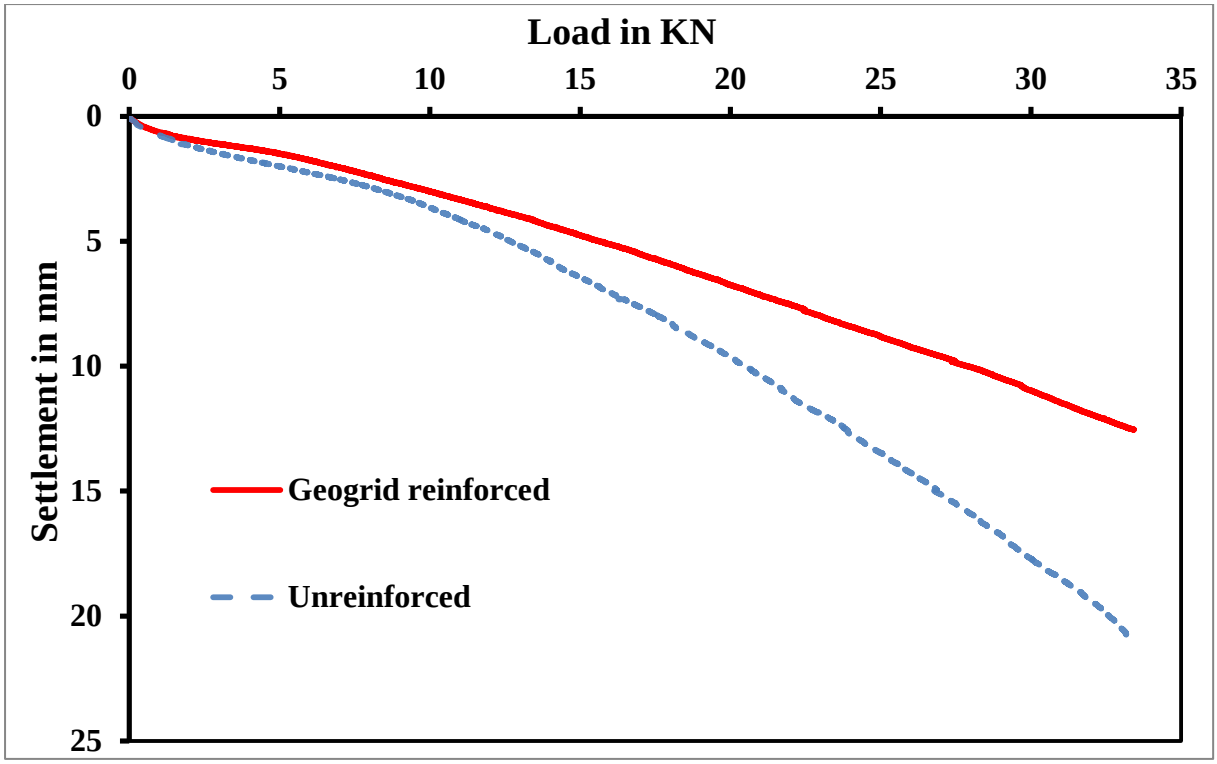

Figure.3.5 (a). Case A - Load vs. settlement for 200mm granular subbase depth

The geogrid acts as a tension membrane, which supports the applied load. This tensioned membrane effect is induced by vertical deformations. The tension developed in the geogrid contributes to support the wheel load and reduces the vertical stress on the subgrade. In our experiment, it is observing that because of membrane effect, reduction in settlement in case of geogrid reinforced granular subbase as compared to unreinforced case.

From Figure.3.5 (b) it shows that load vs settlement curve for the different granular subbase depth. It is observed that percentage of settlement reduction is varied between 7.14% to 41.66% with respect to increase in the depth of granular subbase respectively. The reason for the settlement reduction could be that the planar geogrid also contributes in improving the overall performance of the granular subbase by resisting the downward movement of soil due to the footing penetration.

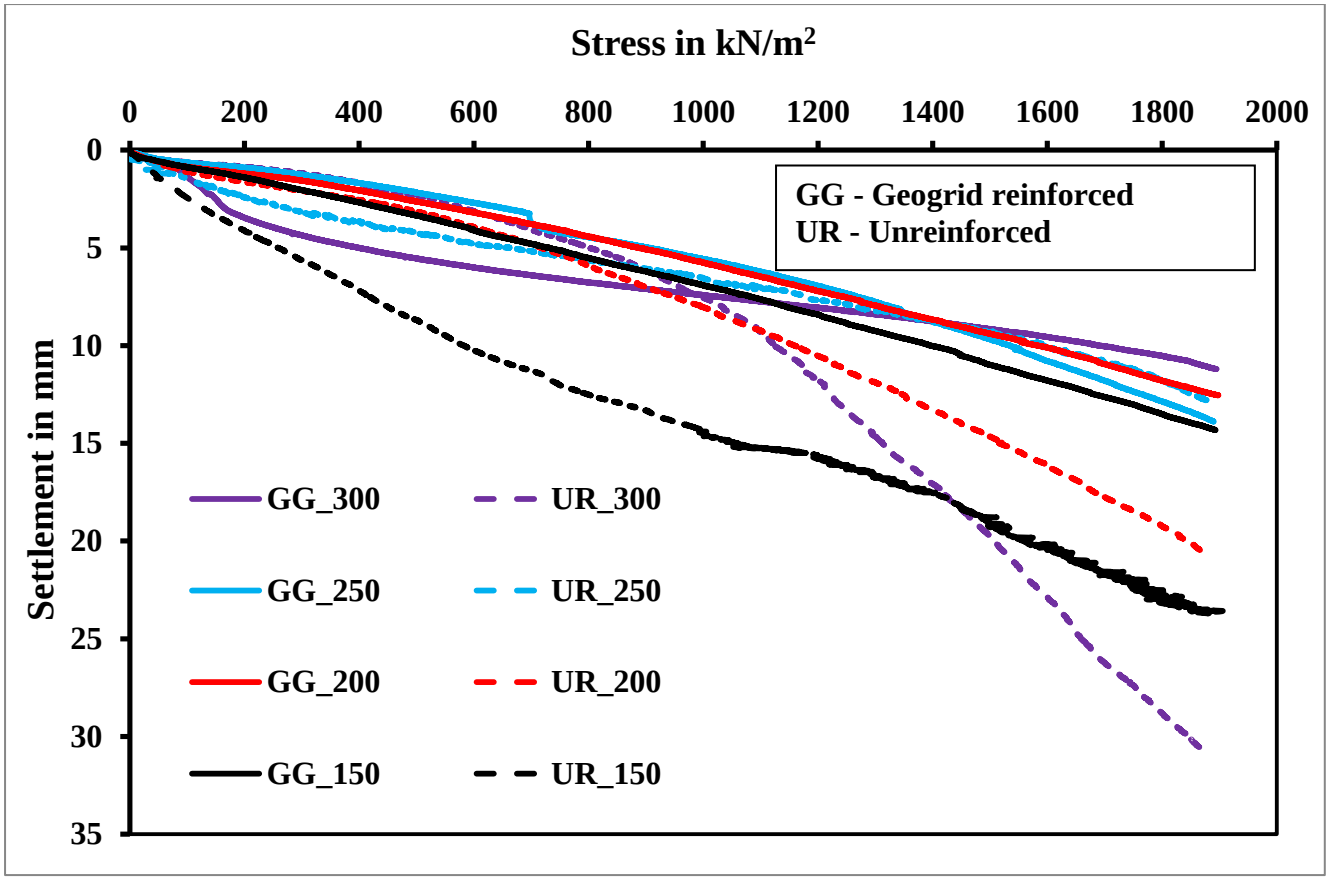

Figure.3.5 (b). Variation of applied stress vs settlement (different depth of granular subbase)

3.7 Strain behaviour of Geogrid

Two strain gauges (SG-1 & SG-2) are placed at the top surface of the geogrid at a predetermined distance and it is clear shown that SG-1 placed at the centre and SG-2 placed at 60mm offset from the centre of footing as shown in Figure.3.4. Fig 3.7 shows the graph between applied stress Vs strain in reinforcement at the edge. In case of 150 and 200 mm depth of the GSB case the strain experienced is less as compared to 250mm case. The load coming from the footing was taken by geogrid upto some point afterwards the load was taken by GSB. But in case of 250 mm the load was taken by geogrid only. So the strain is more in this case, it indicates that the more load was taken by geogrid only. Applied stress versus strain in reinforcement at center is negative at initial stage due to experimental error.

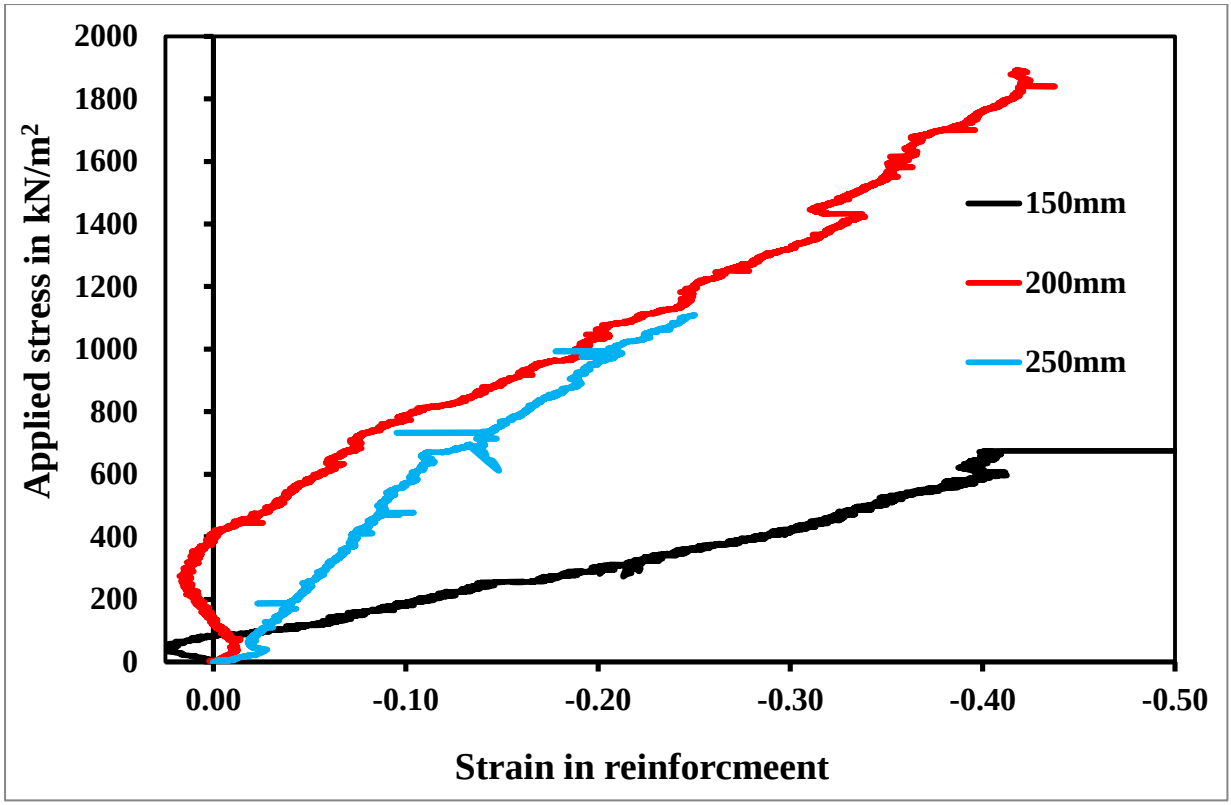

Figure.3.6. Applied stress vs strain in reinforcement (centre)

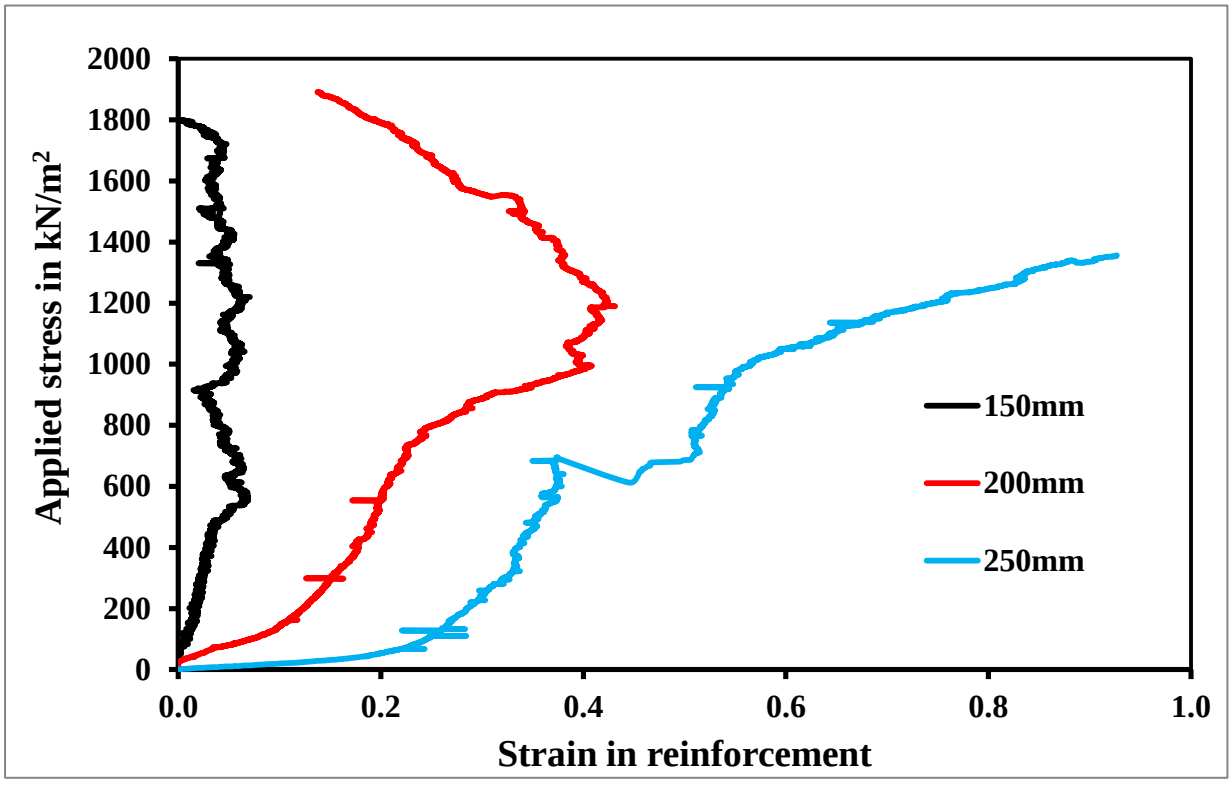

Figure.3.7. Applied stress vs strain in reinforcement (edge).

SG-1 is placed exactly at the centre and SG-2 is placed near to the edge of footing on geogrid surface. In the Figure.3.6 and 3.7., it shows that strain experienced by the geogrid at the centre is less as compared to the strain experienced by the geogrid at 60mm offset from the centre. In Figure.3.7, shows that positive sign indicates tensile behaviour of geogrid reinforcement. The pictorial representation of geogrid after static and dynamic loading was shown in Figure.3.8. In this study as the tests were conducted in laboratory under normal temperature no dummy strain gauge was used to counter the temperature and other effects.

Figure.3.8. Cross section view of the elongated geogrid after the experiment

3.8 Dynamic case

3.8.1 Analysis of result and discussion

In the case of dynamic study, the settlement response was determined corresponding to the number of cycles for each experiment. Figure 3.9 shows the loading pattern for every cycles, load varies in the range of (2000kg)19.62 kN, (2500kg) 24.52 kN, and (3000kg)29.43 kN for every 1000 cycles respectively. Figure 3.9 shows the loading pattern with number of cycles in 2000kg. Similarly for 2500kg, 3000kg the same pattern has followed. Figure 3.10 shows the settlement of the footing after different cycles of loading. The settlement for both unreinforced and reinforced case is presented. It can be seen that settlement increased with increase in depth of granular sub base layer. But the settlement reduced with reinforcement in comparison to unreinforced case irrespective of the number of cycles.

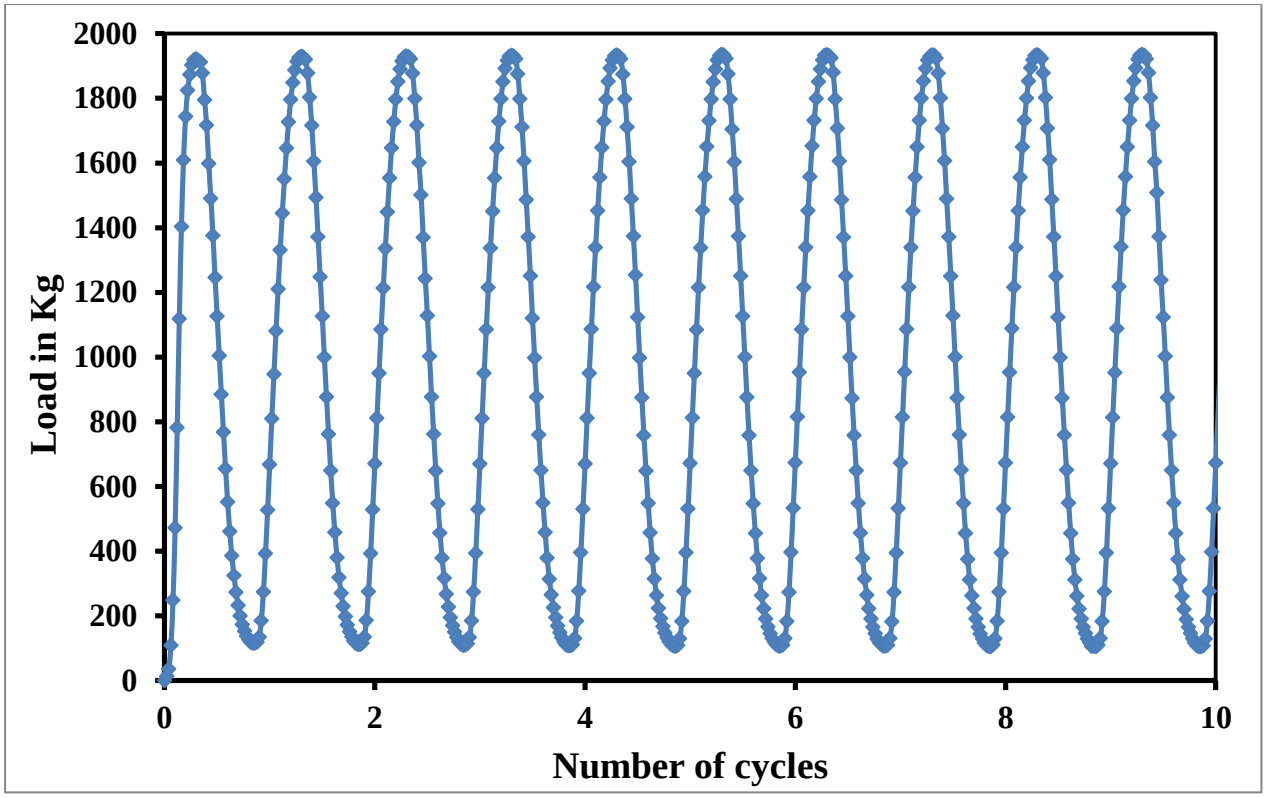

Figure.3.9. Loading pattern with respect to number of cycles

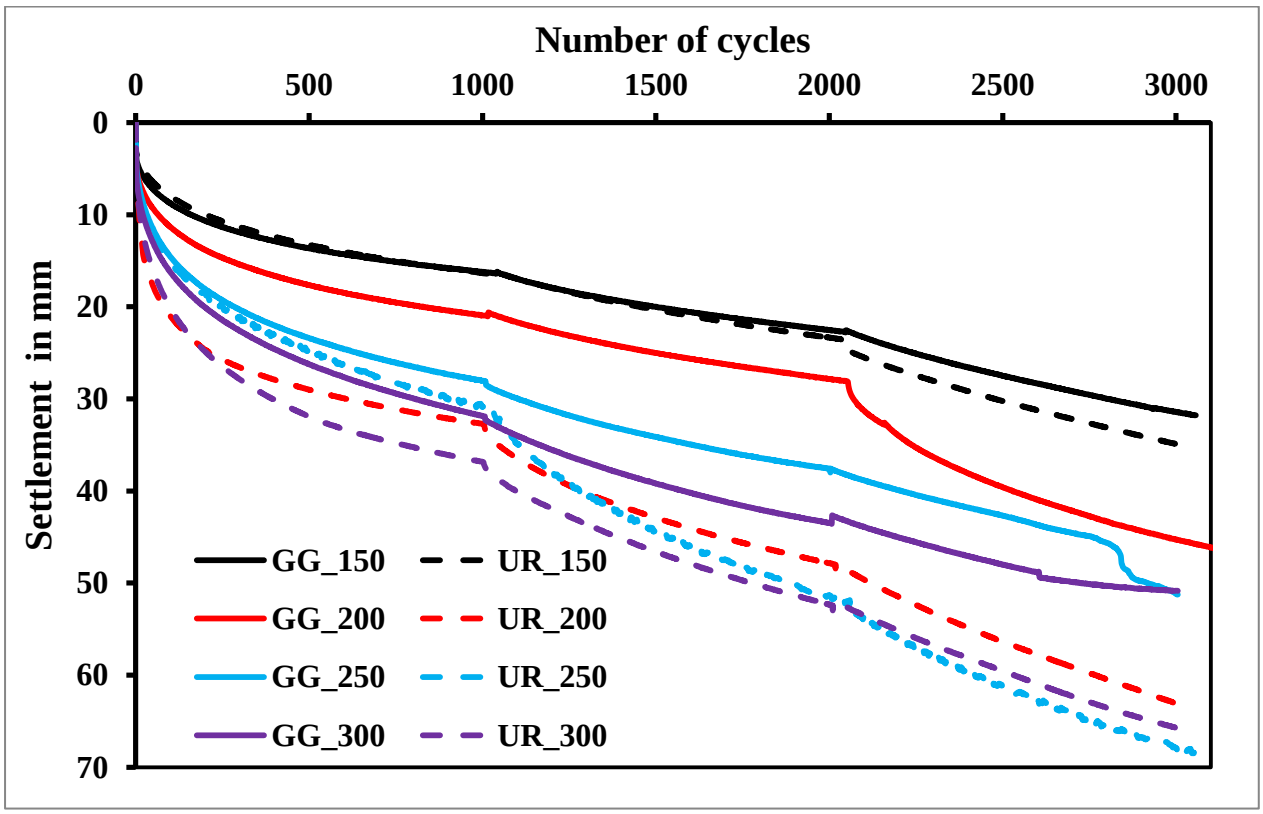

Figure.3.10. Number of cycles vs settlement

In case of 150mm granular subbase settlement is less due to the vertical load is transferring in to the subgrade. It may be the reason, the state of the subgrade material is within the loose state and depth of granular subbase is equal to the width of footing (1B). In the case of 200mm, 250mm and 300mm depth of granular subbase, the vertical load may transfer to the granular subbase at the immediate application of load and gradually it transfers into the subgrade. It may be the one of the reason that the settlement is increasing with respect to the number of cycles by increasing the depth of granular subbase layer.

Hence, it was observed that in case of static load, there is reduction of settlement upto 40% with addition of the reinforcement at the interface of subgrade and subbase. It was also observed that percentage of settlement reduction varied from 7.14% to 41.66% with increase in the depth of granular subbase from 150 to 300mm, showing the importance of subbase layer. But in case of dynamic case settlement increased with increase in depth of granular sub base layer and decreased with provision of reinforcement irrespective of the number of cycles. As the depth of GSB layer increase, the load on the sand increases. During dynamic loading, weight of GSB may be transferring more load to the top the sand, there by densification of sand layer. Hence settlement increases as the depth of GSB layer increases.

CHAPTER 4

NUMERICAL AND ANALYTICAL STUDY

Introduction

Many experimental studies have demonstrated the benefit of using geosynthetics in the roadway base reinforcement (Perkins 2002, Al-Qadi *et al*. 2008). The empirical design methods are often limited to the materials, pavement structures and load levels used in the original experiments. In the present study the experimental results for the static load was analysed using numerical modelling using both finite element method (FEM) and finite difference method (FDM). The commercial software Plaxis ^{2D} uses FEM and in FLAC^{2D} FDM is used. The dynamic test results are compared using empirical method, Giroud and Han (2004).

4.1 Numerical Methods

A brief introduction about the Plaxis^{2D} and FLAC^{2D} is presented in terms of the basic features and their implementations.

4.1.1 Plaxis^{2D}

Plaxis^{2D} is a numerical program based on finite element method which was first invented by1987 at Delft University of Technology in Netherland. This software is intended for analysing two dimensional problems of deformation and stability in geotechnical engineering. The Plaxis^{2D} software contains three sub programs namely the input program, the calculation program and the output program. It performs analysis with either an assumption of plane strain or axis-symmetry with 6-noded or 15-noded triangular elements. In the Finite Element Method, for the measurement of deformations of a soil with their respective state, a mathematical framework is assigned to the soil. These govern the force

displacement relationships and are called material models. In Plaxis^{2D}, there are a number of material models available. However, within the scope of this master's thesis, only the Linear Elastic, Mohr-Coulomb model has been presented in the following sections of this Chapter.

4.1.2 Finite Element Modelling (FEM) procedures

Axisymmetric and Plane strain conditions with two translation degrees of freedom along x axis and y-axis are available in Plaxis^{2D}. However, axisymmetric models are applied only for circular structures with a uniform radial cross section. The loads are also assumed as circular symmetric around the central axis. In the plane strain model the displacements and strains in z-direction are assumed to be zero. But normal stresses in z-direction are considered. The geometry was drawn using geometric lines and standard fixities were then used to define the boundary conditions. The model was created, properties of different soil materials were assigned to material model and finite mesh was generated.

Plaxis^{2D} involves automatic mesh generation. Plaxis^{2D} produces unstructured mesh generation. The mesh generation is based on robust triangulation procedure. Global refinement (to increase the number of elements globally), Local refinement (to increase the number of elements in particular cluster), Line refinement (to increase the element numbers at the cluster boundaries), Point refinement (increasing the element coarseness around the point) are available to obtain the better results. The number of mesh elements considerably affects the results. So sensitivity study on mesh elements for each analysis should be investigated.

Two types of triangular elements are used in the Plaxis^{2D} as 6-node and 15-node triangular elements. Advantages of higher order triangular elements is that they better represent the description of continuous strain-stress variations and good description of a continuous

displacement field compare with relatively few elements. The disadvantages of higher order elements is that the failure loads may be dependent on the mesh and makes poor description of discontinuous stress and strain. In Plaxis^{2D}, the program automatically creates unstructured mesh as there is no possibility of making a so-called structured mesh. The typical mesh for the present study as per PLAXIS^{2D} is shown in Figure 4.1.

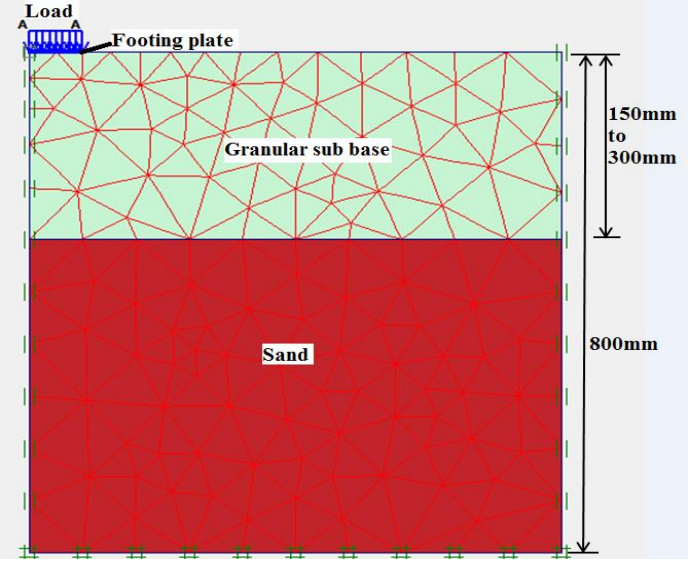

Figure.4.1. A typical mesh generation for the present study in Plaxis^{2D}

4.1.3 FLAC^{2D} (Fast Lagrangian Analysis of Continua)

FLAC^{2D} (Fast Lagrangian Analysis of Continua**)** is an explicit finite difference program especially applicable for Geotechnical and Mining engineering application. It has 11 built-in constitutive models (3 Elastic and 8 Elasto-plastic) for modelling various types of complex problem in soil mechanics. Finite difference method (FDM) discretization is based on the differential form of the Partial Difference Equations to be solved. It utilizes a point-wise approximation to a solution. The domain is discredited into a grid of rectangular cells or nodes. The solution will be obtained at each nodal point. Although FDM is easy to implement and the computing time for each step is fast, the number of steps required for convergence is

high. The FDM code is an explicit two dimensional finite difference program that performs a Lagrangian analysis.

4.1.4 Finite difference modelling (FDM) procedure

The numerical model in FDM is created to simulate the Static load test. A reasonably medium grid was selected to ensure that the displacement contours will be well-defined as it develops. For this analysis the grid size was taken as 50x32. The Linear Elastic Model was taken for sand and Mohr-Coulomb model was taken for granular subbase to analyse the Static load test. The half of the tank was modelled due to axis symmetry of test set up. The size of the model was set with respect to size of tank in each case. Vertical movement is allowed at the bottom of the footing and the tank was fixed at two sides. The model was analysed for both reinforced and unreinforced case. A typical mesh grid as per FLAC^{2D} modelling is shown in Figure 4.2.

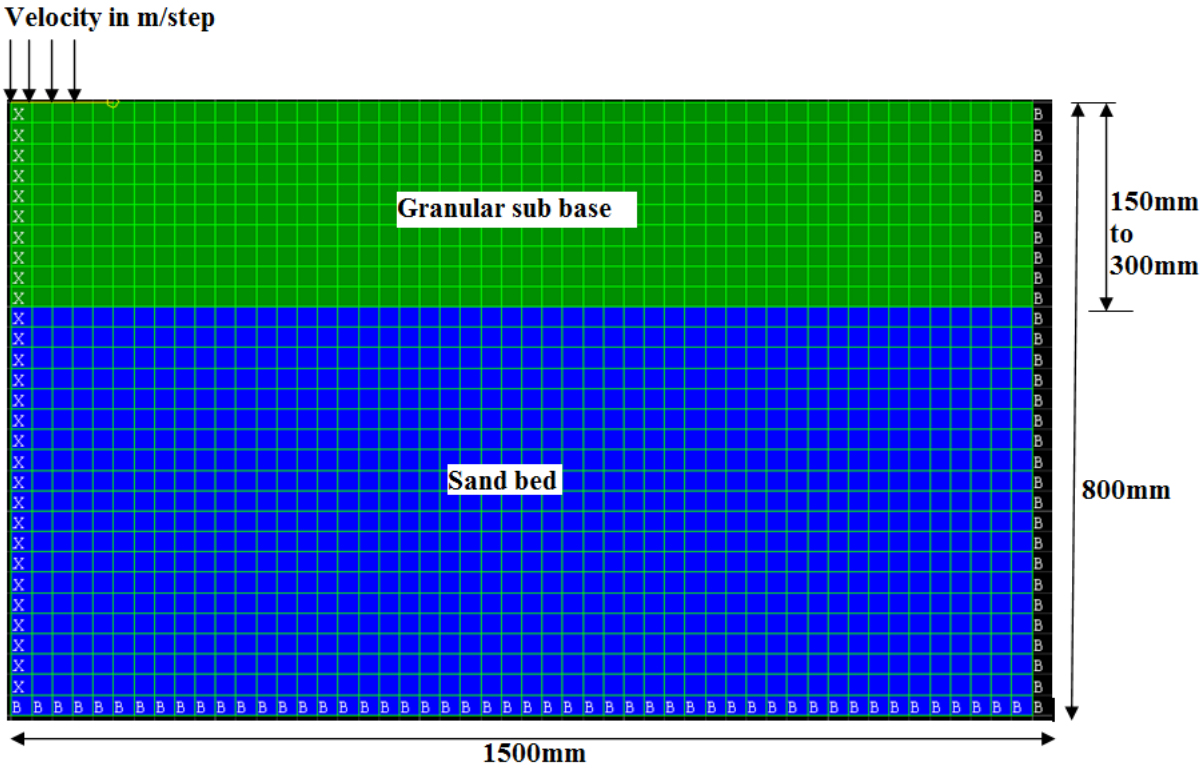

Figure.4.2. A typical mesh generated for the present study by FLAC^{2D}

The Mohr-Coulomb plasticity is applicable for most general engineering studies. This model is used for materials that yield when subjected to shear loading. In this model, the yield stress depends on the major and minor principal stresses and the intermediate principal stress has no effect on it. Hence In the present analysis, Mohr-Coulomb model and linear elastic model for analysis for both Plaxis^{2D} and FLAC^{2D}. The geogrid was modelled as cable element in this study. The elastic modulus of geogrid as taken as 75 Mpa as obtained from experiment.

4.1.5 Mohr-Coulomb material model

The failure occurs at that point when the shear stress at a point on any plane within a soil becomes equal to shear strength. The shear strength expresses as a linear function with cohesion c, angle of shearing resistance(ϕ) and normal stress at failure (σ_f'). The expression of shear strength in terms of effective stress as

$$\tau_{f=c'+\sigma_f' \tan \emptyset'} \tag{4.1}$$

At stress ranges when the yield occurs, the soil material is elastic in its behaviour. As a critical combination of shear stress and effective normal stress develops, the stress point will coincide with the failure envelope and a perfectly plastic material behaviour is assumed.

The Mohr-Coulomb failure criterion can be expressed as

$$\sigma_1' = \sigma_3' \tan^2\left(45 + \frac{\emptyset'}{2}\right) + 2c' \tan\left(45 + \frac{\emptyset'}{2}\right) \tag{4.2}$$

The main features of the Mohr-Coulomb material model includes

- It obeys the Hook's law
- Linear elastic perfectly plastic yield envelope

- Five input parameter such as Young's modulus, Poisson's ration, cohesion, Friction angle and Dilatancy angle are required.

4.1.6 Properties

The basic properties of the sand and granular subbase were taken from Burt G. Look. (2007). These values are mentioned as below. The inputs for Plaxis ^{2D} is shown in Figure 4.1 and that for FLAC ^{2D} is shown in Table 4.2. As in case of Plaxis^{2D}, cohesion value of '0' shows numerical error, a small value of 1 kPa is considered for sand. The elastic modulus of sand and Granular subbase are varied in the range as per literature to find good agreement with the experimental values. Hence, different values of elastic modulus are taken for Plaxis^{2D} and FLAC^{2D}.

Table.4.1. Input model parameter used in Plaxis^{2D}

Input parameters	Elastic Modulus (Mpa)	Cohesion (kPa)	Angle of fiction (Degree)	Mass-density (kg/m^3)	Poisson's ratio
Sand	13	1	31	1800	0.25
Granular subbase	65	10	40	2100	0.3

Table.4.2. Input model parameter used in FLAC^{2D}

Input parameters	Elastic Modulus (Mpa)	Cohesion (kPa)	Angle of fiction (Degree)	Mass-density (kg/m^3)	Poisson's ratio
Sand	22	0	31	1800	0.25
Granular subbase	85	10	40	2100	0.3

4.1.7 Result and Analysis

The experimental results have been validated with numerically by using the Plaxis^{2D} and FLAC^{2D} as per the material properties describer in the previous section are presented in Figures, 4.3-4.6 for different thickness of the GSB layer. For GSB layer of 150mm, 200mm and 250mm thickness, for both the unreinforced and reinforced case the numerical results as per FLAC^{2D} match better to the experimental result than Plaxis^{2D} result. Whereas, for the 300mm thick GSB layer Plaxis ^{2D} results close to experimental results.

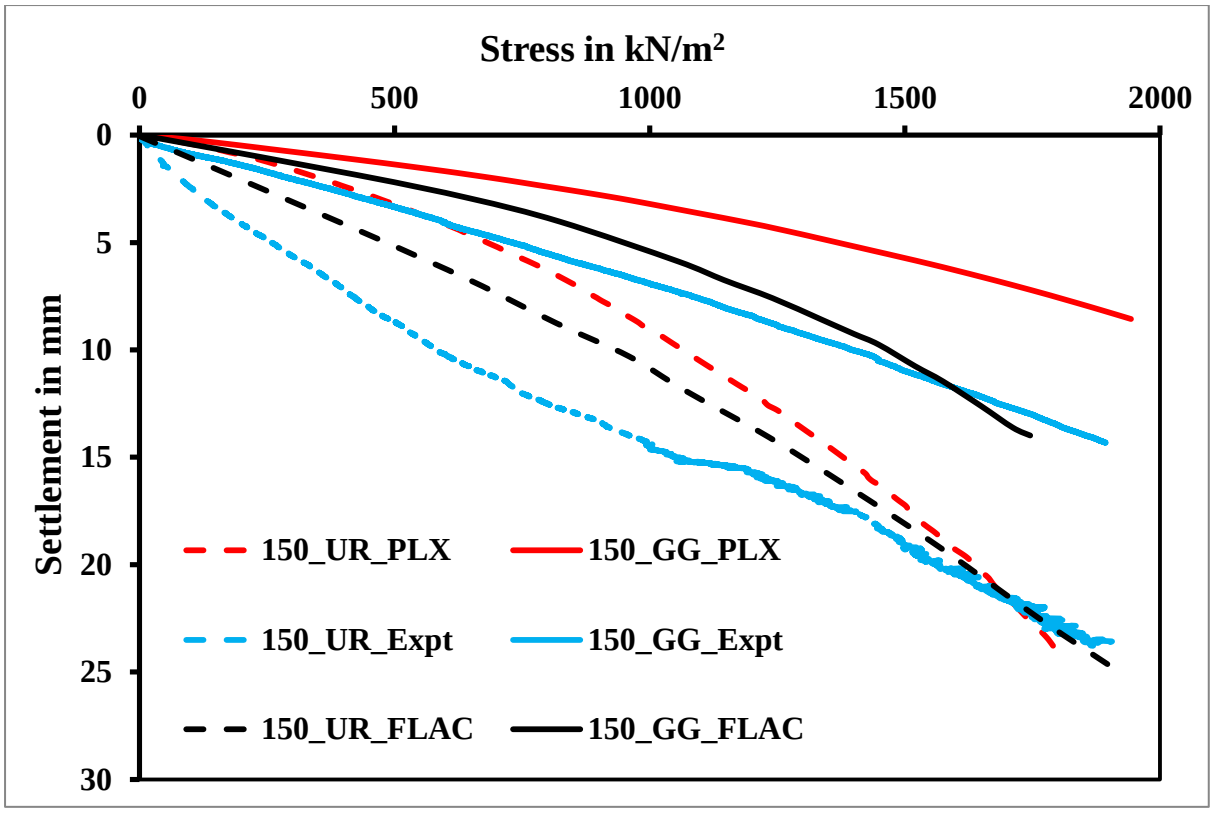

Figure.4.3. Stress vs settlement curve for 150mm granular subbase

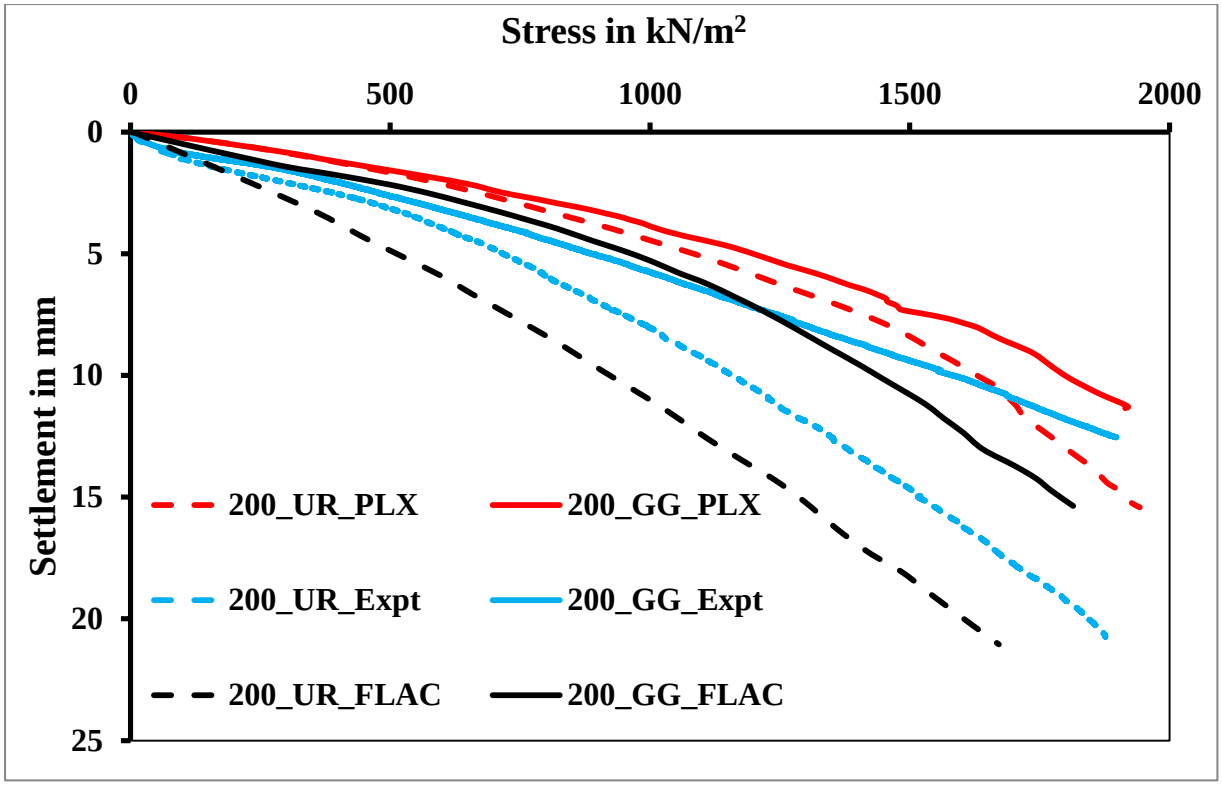

Figure.4.4. Stress vs settlement curve for 200mm granular subbase

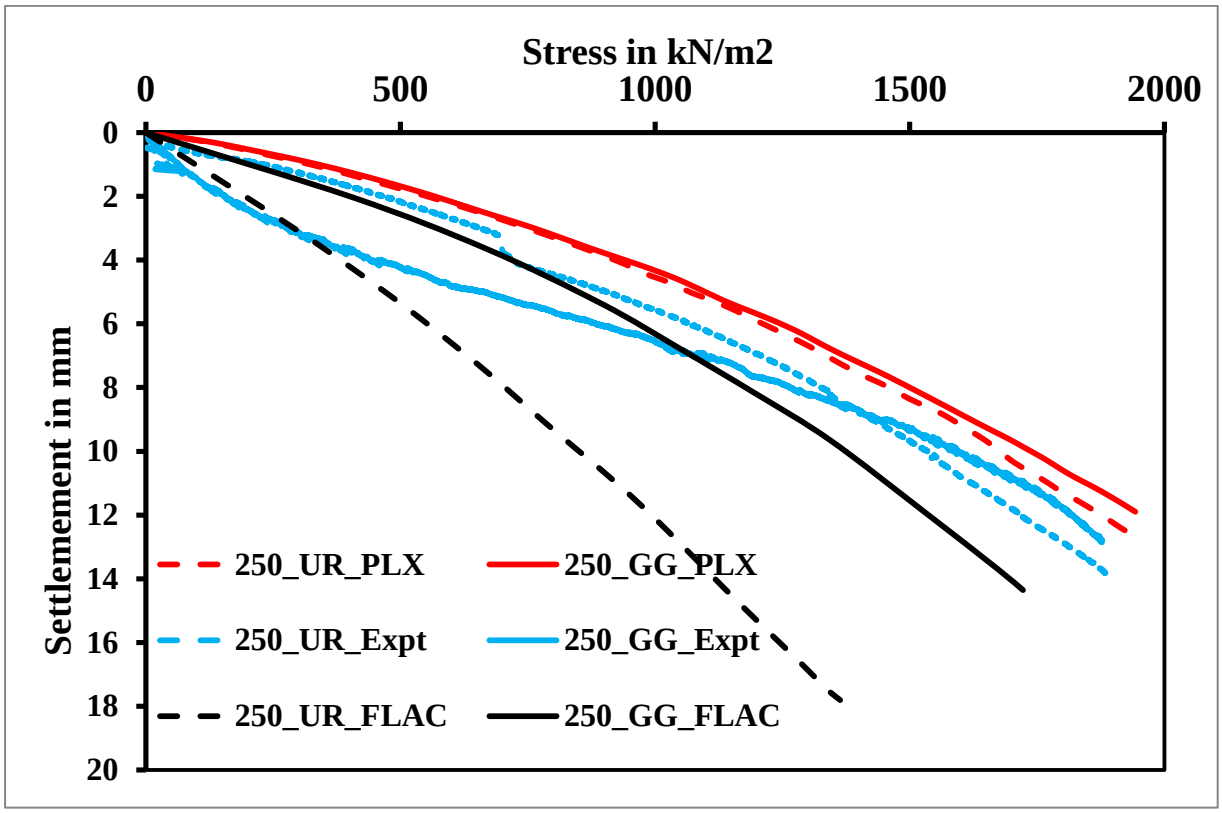

Figure.4.5. Stress vs settlement curve for 250mm granular subbase

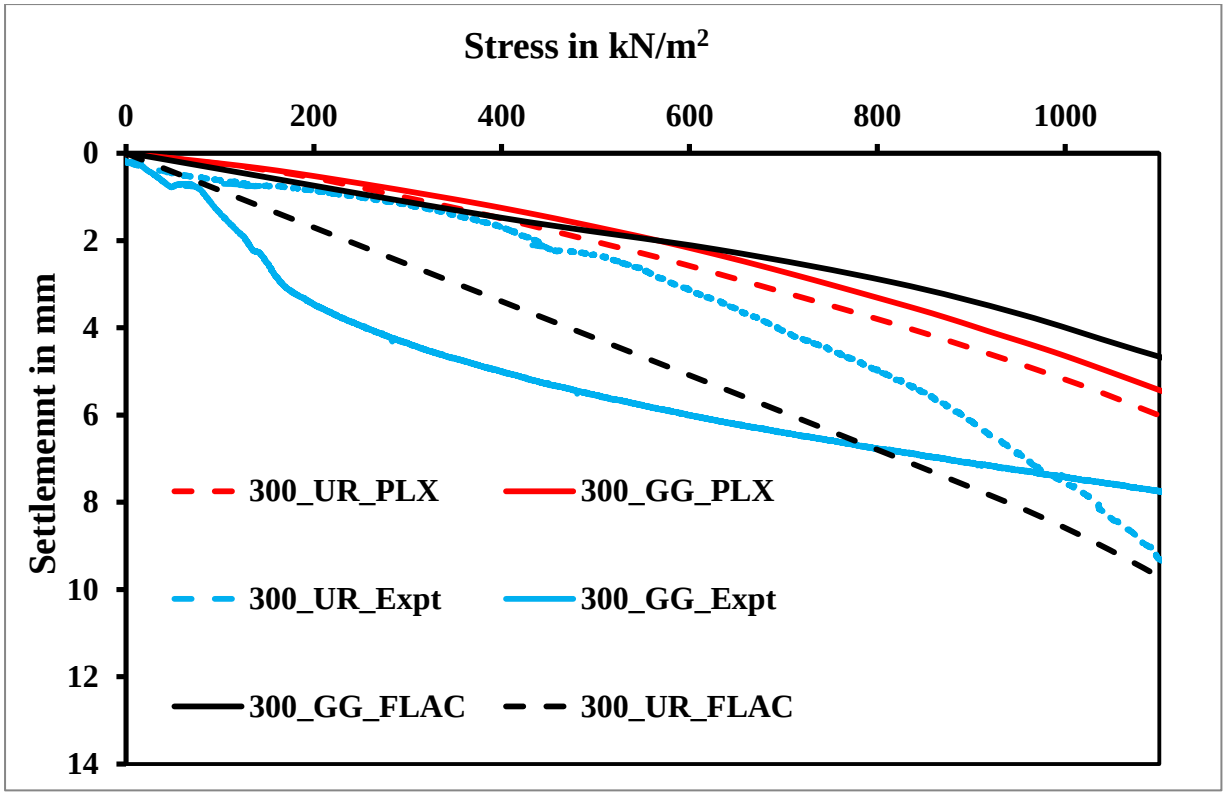

Figure.4.6. Stress vs settlement curve for 300mm granular subbase

Table.4.3. Comparison of experimental and numerical method results

Applied stress	**Depth of granular subbase**	**Cases**	**Variation in percentage (%)**	
			Experimental and Plaxis^{2D}	**Experimental and FLAC^{2D}**
1000kN/m^2	150mm to 300mm	Unreinforced	25% - 30%	8.6% - 35%
		Geogrid	7% - 30%	7% - 20%

It was observed that unreinforced case there is wide variation in FLAC^{2D} (8.6 to 35%) with that of experimental results in comparison as shown in Table 4.3. Whereas, for the reinforced case less variation was observed with FLAC ^{2D} (7-20%) than that of Plaxis ^{2D} (7-30%). It may be mentioned here that the model parameters are considered based on the literature value and hence, the variation need to be checked with actual parameters of the used material.

4.2 Evaluation of design methods of geogrid reinforced unpaved roads by Grioud and Han equation

Giroud and Han's equation is a theoretically based design method for finding out the thickness of the base course of unpaved road by considering the important parameter such as distribution of stress, strength of base course material, interlock between geosynthetic and base course material and geosynthetic stiffness in addition which has been also considered as earlier methods (Giroud and Noiray 1981, Giroud et al. 1985) like traffic volume, wheel loads, tire pressure, subgrade strength, rut depth, and influence of the presence of a reinforcing geosynthetic geotextile or geogrid on the failure mode of the unpaved road.

Design parameters

During calculation of the settlement value from Giroud and Hans's equation, some of the design parameters are used and those parameters are mentioned below.

4.2.1 Geometry of unpaved structure and Traffic

The base course has a uniform thickness. It is assumed that only one layer of geogrid is used. This layer of geogrid is assumed to be placed at the base course/subgrade soil interface. In our present study a minimum base course thickness of 0.15 m was taken in this paper. This minimum thickness was considered to ensure the constructability of the base course and to minimize disturbance of the subgrade soil during trafficking. Another reason for using a minimum base course thickness was to provide sufficient anchorage for the geogrid.

Channelized traffic is characterized by the number of passes (N), of a given axle during the design life of the structure. For Dynamic test, numbers of passes were taken as 3000 cycles.

4.2.2 Axles and loads

Different type of axle load are exist, single axle and double axles etc. and in present study it will be single axle load case. In case of Dynamic test axle load vary from 19.62 kN to 29.43 kN and it is provided in the particular format i.e. first 1000 cycles followed by the 19.62 kN, remaining every thousand cycles followed by 25.54 kN and 29.43 kN respectively. According Giroud and Han's equation axle geometry as shown in the Figure.4.7.

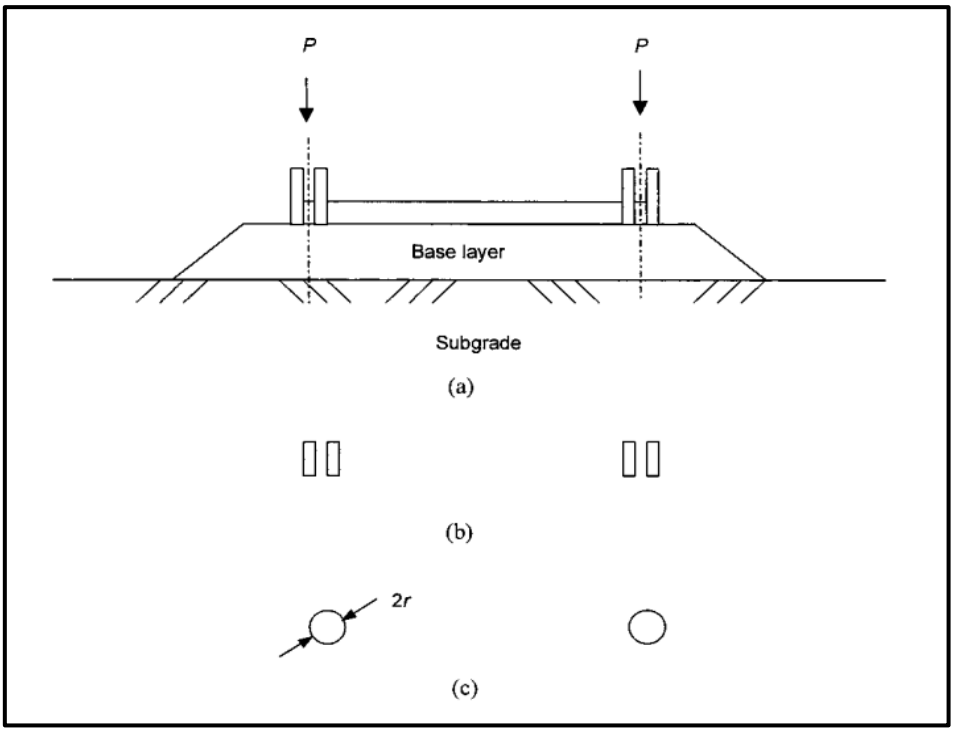

Figure.4.7. Vehicle axle and contact area: (a) Geometry of vehicle axle with dual wheels; (b) Tire contact areas; and (c) equivalent contact area used in analysis (Giroud and Han 2004).

$$P = pA \tag{4.3}$$

Where,

P= Wheel load (kN);

p = Tire contact pressure between the each tire and base course.

A= Tire contact area (m^2) , $A = \pi r^2$

$$r = \sqrt{\frac{P}{\pi p}} \tag{4.4}$$

For American British standard axle load (P_A=80 kN, i.e. P=40 kN)

Tire inflation pressure of 550 Kpa and radius of contact area is about the 0.15m.

Rut depth and serviceability criterion (f_s)

Ruts generates due to the traffic, which was observed at the surface of the base course. A failure criterion defined by the allowable rut depth of 75 mm was adopted by the US army Corps of Engineers. It is widely used for unpaved road. According to AASHTO design guide lines consider allowable rut depths from 13 to 75mm and sometimes used, such as 100mm.

4.2.3 Base course material

According to AASHTO (1993), the relationship between modulus of the base course and the CBR can be expressed as follows:

$$E_{bc} = f_{EBC} CBR_{bc}^{0.3} \tag{4.5}$$

Where,

E_{bc} = base course resilient modulus (MPa)

CBR_{bc} = base course California bearing ratio

f_{EBC} = factor equal to 36MPa (for E_{bc} in MPa)

4.2.4 Bearing capacity mobilization coefficient (m)

The bearing capacity mobilization coefficient depends upon the thickness of base course. If the base course thickness is more than zero bearing capacity mobilization coefficient is less than 1 and base course thickness is zero the bearing capacity mobilization coefficient is 1.

$$m = \left(\frac{s}{f_s}\right)\left\{1 - \xi exp\left[-\omega\left(\frac{r}{h}\right)^n\right]\right\} \quad (4.6)$$

Where,

s = allowable rut depth(mm), f_s = factor equal to 75mm

4.2.5 Subgrade material

The value of undrained cohesion of subgrade soil (c_u) can also be approximately deduced from the CBR value of the subgrade soil for CBR_{sg} (less than 5) using the following relationship Giroud and Noiray 1981.

$$c_u = f_c CBR_{sg} \quad (4.7)$$

Where, $f_c = \text{constant}(30kPa)$

In case of laboratory soaked CBR test for sand, the stress has observed 1734 kN/m^2 for settlement of 5mm. Similarly for corresponding settlement of 5mm has considered in the experimental large scale plate load test in the range of from 258 kN/m^2 to 799.515 kN/m^2. From both test results it has clearly shown that, stress observed in the case of laboratory CBR test is more as compared to the experimental large scale plate load test, because it may due to the confining pressure experienced by the laboratory CBR test is more as compared to large scale plate load test. The soaked CBR value has found for sand is 10.33%. Similarly for experimental large scale plate load test, The equivalent CBR value determined in experimental large scale plate load test in the range of 1.46% to 4.61% with respect to soaked CBR value. Hence, in analytical study, we have considered the CBR value of subgrade is 3%.

Stresses on subgrade soil

For find outing the normal stress at the interface between base course and subgrade soil was given by the following equation.

$$P_i = \frac{P}{\pi(r + h\ tan\ \alpha)^2} \tag{4.8}$$

$$h = \frac{r}{tan\ \alpha}\left(\sqrt{\frac{P}{\pi r^2 P_i}} - 1\right) \tag{4.9}$$

Where,

P_i = distributed normal stress at interface between base course and subgrade (kPa)

α = stress distribution angle

r = radius of the equivalent contact area

4.2.6 Evaluation of wheel load in pavement

The distributed normal stress (p_i), at the interface between base course and subgrade soil needs to meet the following requirement in order to prevent subgrade soil failure.

$$P_i \leq mN_c c_u \tag{4.10}$$

The bearing capacity mobilization coefficient ($0 < m \leq 1$) accounts for the fact that only a fraction of the bearing capacity of the subgrade soil is mobilized. Combining Equations.

$$h \geq \frac{r}{\tan \alpha}\left(\sqrt{\frac{P}{\pi r^2 m N_c c_u}} - 1\right) \tag{4.11}$$

Where,

N_c = bearing capacity factor

c_u = undrained cohesion of subgrade soil (30 kPa)

The bearing capacity factor in this study, for unreinforced unpaved roads is 3.14; for geosynthetic reinforced unpaved roads is 5.14 and 5.71. The bearing capacity mobilization coefficient for an allowable rut depth of 75 mm is equal to 1.0 when the base course thickness is zero and decreases with increasing values of the thickness of the base course. Another equation suggested for the bearing capacity mobilization coefficient, when the serviceability criterion is an allowable rut depth of 75 mm. The constants in the following equation were obtained by calibrating the field wheel load tests based on cyclic plate load tests.

$$m = 1 - \xi xp\left[-\omega\left(\frac{r}{h}\right)^{n}\right] \tag{4.12}$$

Where,

m = mobilization coefficient

r = radius of the equivalent tire contact area (m)

h = required base course thickness (m)

ξ =1, ω = 1 and n = 2 (determined through calibration of field tests).

In cases where the rut depth may not be 75 mm, the following equation can be used to determine the mobilization coefficient:

$$m = \left(\frac{s}{f_s}\right)\left\{1 - \xi exp\left[-\omega\left(\frac{r}{h}\right)^{n}\right]\right\} \tag{4.13}$$

Where,

s = allowable rut depth (mm) and f_s = factor equal to 75mm.

The design equation for wheel load is given as:

$$P = \pi r^2 \left(\frac{s}{f_s}\right)\left\{1 - 0.9exp\left[-\left(\frac{r}{h}\right)^2\right]\right\} N_c c_u \times \left[1 + \frac{\left(\frac{h}{r}\right)[1 + 0.204(R_E - 1)]}{0.868 + \left(0.661 - 1.066J^2\left(\frac{r}{h}\right)^{1.5} Log\ N\right)}\right]^2 \quad (4.14)$$

Where,

N = number of passes of axle

R_E = modulus ratio of base course to subgrade soil

J = aperture stability modulus of geogrid

P = tire contact pressure

s = allowable rut depth, f_s = factor equal to 75mm rut depth

ξ and ω= constants

The experimental dynamic test was validated with the Giroud and Han's equation. Giroud and Han's equation was used for calculating the settlement for corresponding number of cycle, by considering the properties of granular subbase and subgrade, geogrid properties and wheel load, number of repetition as given in below Table.4.4.

Table.4.4. Giroud and Han's equation parameters

Parameters	**Value**
Bearing capacity factor (N_c)	3.14 for Unreinforced case
	5.14 for Geotextile case
	5.71 for Geogrid case
Number of passes of axles(N)	Varied between 500 to 3000
Thickness of base course (h)	Varied between 150m to 300mm
Aperture stability modulus of geogrid (J)	0.65m N/◦
Number of passes of axles (N)	0 to 3000
Undrained cohesion of subgrade soil (c_u)	90 kPa
Modulus ratio of base course to subgrade soil (R_E)	5

4.2.7 Result and analysis

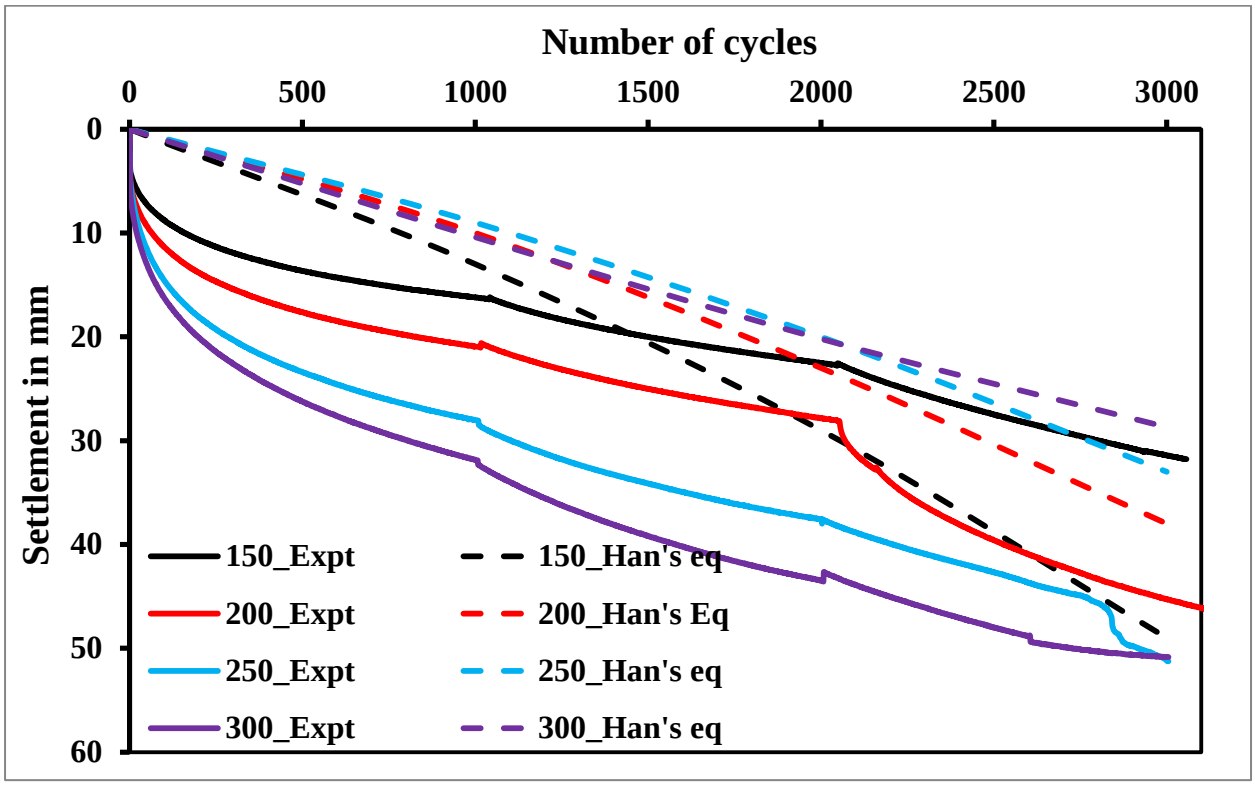

Figure.4.8. Number of cycle vs settlement

In the case of dynamic test, the settlement increases as the depth of granular subbase increases in the experimental case. It may be the reason due to the rearrangement particles of granular subbase material when repeated load applied. But in the case of empirical method (Giroud and Han's method) the settlement decreases as the depth of granular subbase increases as shown Figure.4.8. Hence reverse trends were observed between present experimental results and the existing empirical method.

CHAPTER 5

DEVELOPMENT OF PREDICTION MODELS USING ARTIFICIAL INTELLIGENCE TECHNIQUES

Introduction

In this present chapter an effort has been made to develop prediction model separately for static and dynamic load cases for reinforced pavement resting on granular material. Two recently developed artificial intelligence techniques, genetic programming (GP) and multivariate adaptive regression spline (MARS) have been used to develop the prediction models. Different statistical performances criteria like correlation coefficient (R), Nash's coefficient of efficiency (E) (Das and Basudhar 2006), average absolute error (AAE), and maximum absolute error (AAE), root mean square error (RMSE) are used to compare the developed prediction models. As both the methods are new to geotechnical engineering, a brief introduction about GP and MARS and their applications in geotechnical engineering has been presented. Then prediction models for evaluating the performance of reinforced pavement in flexible pavement in terms of settlement and bearing capacity is presented using GP and MARS have been addressed. A sensitivity analysis is also made to identify important input parameters affecting the settlement and bearing capacity of the developed model.

5.1 Genetic Programming (GP)

Genetic Programming is a pattern recognition technique where the model is developed on the basis of adaptive learning over a number of cases of provided data, developed by Koza (1992). It mimics biological evolution of living organisms and makes use of the principles of genetic algorithms (GA). In traditional regression analysis the user has to specify the structure of the model, whereas in GP, both structure and the parameters of the mathematical model are evolved automatically. It provides a solution in the form of a tree structure or in the form of a compact equation using the given dataset. A brief description about GP is presented

for the completeness, but the details can be found in Koza (1992). The nodes of the GP have created by functional set or terminal set in a GP tree. A functional set includes four types of parameter (i) arithmetic parameter, (ii) logical expression (ex-IF, THE), (iii) Boolean operators (AND, OR) and (iv) mathematical functions (tan, sec, in, cos). The GP tree comes as different size and shape.

Initially a set of GP trees, as per user defined population size, is randomly generated using various functions and terminals assigned by the user. The fitness criterion is calculated by the objective function and it determines the quality of each individual in the population competing with the rest. At each generation a new population is created by selecting individuals as per the merit of their fitness from the initial population and then, implementing various evolutionary mechanisms like reproduction, crossover and mutation to the functions and terminals of the selected GP trees. The new population then replaces the existing population. This process is iterated until the termination criterion, which can be either a threshold fitness value or maximum number of generations, is satisfied. The best GP model, based on its fitness value that appeared in any generation, is selected as the result of genetic programming. A brief descript on various evolutionary mechanisms in GP are presented below.

Four steps need to solve a GP problem which is presented below.

Initial Population

The first step is to generate the initial population by randomly generating functions and terminals in GP tree. The performance of each structure measures by fitness value.

Reproduction

In this stage some proportion of initial population has selected and copied to the next generation. For choosing this population, so many sub steps are there among those routes

wheel selection is one. The trees having higher fitness value, more probability for choosing for the next generation.

Crossover

In this stage two trees are selected from each population and one node is selected randomly chosen within each of the two trees and sub-trees under the selected nodes are swapped to generate two offspring which belongs to new population.

Mutation

In the last stage in GP, when the node of the one tree is replaced by another tree with the functional and terminal set, there is one principle is applicable i.e. A functional node can be replaced by only a function node and same as the terminal node.

Gandomi and Alavi (2012b) developed a variant of GP called multi-gene GP (MGGP) and has been used for liquefaction classification model using the CPT database. Muduli et al. (2013) used MGGP for prediction of uplift capacity of caisson and found to more efficient compared to ANN and SVM model.

5.1.1 Multi Gene Genetic Programming (MGGP)

It is a variant of GP intended to generate a mathematical model corresponding input and output data with multi-gene behaviour. In the GP we have considered a single tree expression but in MGGP, the numbers of genes are formed having tree expressions. Figure.15. shows an example of MGGP model, this model predicts the output variable using four input variable. Each gene is having nonlinear terms. The maximum number of allowable genes (G_{max}) and maximum tree depth (d_{max}) may have specified by user. In the MGGP model the initial population are created individuals randomly containing GP trees by varying number of gene 1 to(G_{max}). MGGP also provides six methods of mutation of genes (Gandomi and Alavi

2012a). The user has specified the probabilistic of various evolved mechanism in MGGP in such a manner that the developed model should effective and the sum of the probability of crossover event, reproduction event, mutation event, should be equal to 1. The general form of proposed GP model can be presented as

$$Q_p = \sum_{i=1}^{n} F[x, f(X), b_i] + b_0 \quad (5.1)$$

Where,

F= the function created by the GP

X = vector of Input variables

5.2 Multivariate Adoptive Regression Spline (MARS)

Multivariate adaptive regression splines (MARS), as the name suggests is an adaptive regression technique used to fit the relationship between a set of input variables and an independent variable. MARS uses a non-parametric regression technique for prediction of the dependent variable, i.e., no prior assumption is made about the relationship between the dependent and independent variables. This relation is constructed from a set of coefficients and basis functions determined entirely from the data in hand. Thus, MARS is advantageous over other statistical techniques for problems with a greater amount of input data. Because of taking capacity of large number of data it is very helpful for doing the high dimensional problem. In this method regression input data is used to construct this relation and forms between some sets of coefficients and basis functions. MARS lies in its ability to estimate the contributions of the basis functions so that both the additive and the interactive effects of the predictors are allowed to determine the response variable. In this present study MARS has given the relation between input (x) and output variable (y) by the following equation

$$y = \beta + \sum_{i=1}^{n} B_x \alpha_x(x) \tag{5.2}$$

Where,

β = interceptor parameter

B_x = basis Function

α_x = coefficient of basis function

x = input variables

y = predicted output (Q)

Two stepped algorithm is used to model the MARS function

(i) Forward stepwise algorithm

(ii) Backward stepwise algorithm

5.2.1 Forward stepwise algorithm

This algorithm searches for the constant basis function, for giving a linear better fit equation. The process stops when a user specified values means number of iteration steps reached. At the end of the process, a large expression obtains and it over fits the data. For considering the over fit of data we look over to backward stepwise algorithm.

5.2.2 Backward stepwise algorithm

The main aim of this algorithm is to decrease the complexity of the model without degrading the fit to the data as well as to minimise error. The backward stepwise algorithm used to remove the model basis functions that contribute to the smallest increase in the residual

squared error at each stage of the iteration step, defined as α, where α is known as complexity of the estimation of the model. Generalized cross-validation is used to calculate α (complexity of the model).

5.3 Development of prediction model for reinforced bed for static load case

In this section development of prediction model for bearing capacity of reinforced bed for static case is presented.

5.3.1 Database and Processing

The database used for the present study is presented in Table 5.1. Based on the data base presented in this Table 5.1, the input variables are { t, S_e ,E_{sg}, E_{sb}}, where t=thickness of the granular subbase, S_e = Settlement of the circular footing, E_{sb} =Elastic modulus of base course, E_{sg} = Elastic modulus of subgrade and output is the bearing capacity**.** In the present case the data was generated by doing numerical analysis in FLAC software. As FLAC is settlement control method, the database is obtained by varying the elastic modulus of subgrade, base course and settlement to get corresponding load at each case. Out of the mentioned 40 data, 28 data are selected for training and remaining 12 data are used for testing the developed model. The training data is presented in Table.5.1 and the testing dataset in Table.5.2. The data were normalized in the range 0 to 1 to avoid the dimensional effect of input parameters for MARS. In the GP modelling normalization or scaling of the data is not required.

Table.5.1. Training data prediction of bearing capacity

Thickness of GSB (t) (mm)	Settlement of the pavement (S_e) (mm)	Elastic modulus of subgrade (E_{sg}) (Mpa)	Elastic modulus of subbase (E_{sb}) (Mpa)	Q_f (Predicted Bearing Capacity using FLAC) (kN/m^2)
200	20	31	85	3775
150	7	16	60	700
250	12	22	70	1900
150	5	13	55	425
200	17	28	80	2950
250	5	13	55	550
150	2	10	50	70
150	12	22	70	1320
150	20	31	85	3400
300	10	19	65	1570
200	15	25	75	2400
150	17	28	80	2650
300	20	31	85	4400
250	17	28	80	3200
200	5	13	55	485
250	15	25	75	2600
100	2	10	50	70
250	2	10	50	75
300	5	13	55	615
150	10	19	65	1140
100	5	13	55	370
100	12	22	70	1500
200	7	16	60	800
200	10	19	65	1300
300	17	28	80	3500
300	2	10	50	71
100	20	31	85	3300
250	20	31	85	4100

Prediction model as per MARS

In this section the prediction model as per MARS is presented and the GP model is presented in the next section. As we know the as the number of basic function increases the complexity of the model increased. Keeping in this in mind, 8 basic functions are used in present study.

Table.5.2. Testing data prediction of bearing capacity

Thickness of GSB(mm) (t)	Settlement of the pavement (S_e) (mm)	Elastic modulus of subgrade (E_{sg}) (Mpa)	Elastic modulus of subbase (E_{sb}) (Mpa)	Q_f (Predicted Bearing Capacity using FLAC) (kN/m^2)
300	15	25	75	2800
100	10	19	65	1020
100	17	28	80	2400
200	2	10	50	70
150	15	25	75	2140
300	12	22	70	2100
250	10	19	65	1430
100	15	25	75	1920
250	7	16	60	890
100	7	16	60	615
300	7	16	60	980
200	12	22	70	1720

The coefficients of different basis functions produced for the developed MARS mode, model equations can be written using the obtained coefficients and basis functions as presented in Equation 5.2 as follows

$$Q_p = 0.5 - 0.15(0.75 - t) + 0.46x(E_{sb} - 0.57)(t - 0.25) + 1.063(S_e - 0.72) - 0.78(0.72 - S_e) + 0.563(0.72 - S_e)(0.42 - E_{sg})(0.75 - t) \quad (5.3)$$

Where,

$(0.75- t) = \max (0, 0.75 - t)$

$(E_{sb}-0.57) = \max (0, E_{sb}-0.57)$

$(S_e -0.72) = \max (0, S_e-0.72)$

$(0.72- S_e) \max (0, 0.72-S_e)$

$(0.42-E_{sg}) = \max (0, 0.42 - E_{sg})$

Prediction model as per MGGP

In the present study each individual in the population consists of more than one gene and each gene is a traditional GP tree. Here, function set used include: +, ×, ÷, -, and exp (.). As discussed earlier in MGGP procedure first a number of potential models are evolved at random. Each model is trained and tested using the training and testing cases respectively. The fitness of each model is determined by minimizing RMSE between the predicted (Q_p) and actual (Q_m) value of the output variable as the objective function.

The best Q_p model was obtained with population size of 2000 individuals and 150 generations with reproduction probability of 0.05, crossover probability of 0.85, mutation probability of 0.1 and with tournament selection. In GP model development it is important to make a trade off between accuracy in prediction of Q_p and complexity of the model equation which is achieved by proper selection of number of genes and depth of GP tree. In this study optimum result was obtained with maximum number of genes as two and maximum depth of GP tree as four. The developed MGGP model can be described as above equation as shown in below.

$$Q_p = 0.0679t + 4.47E_{sb} - 0.0496\left(0.088\mathrm{Se} + \frac{\mathrm{t}}{E_{sb}}\right)(2t - tS_e + 4.576S_eE_{sg} - 238 \qquad (5.4)$$

The variations of predicted and observed values of Q_p for training and testing data as per MARS modelling are shown in Figure 5.1, along with line of equality. It can be seen that there is less scattering in the data. Similarly, the variation of predicted and observed values of Qp for training and testing data as per GP modelling is shown in Figure 5.2. In comparison to MARS modelling, there is less numbering scattering in data as per

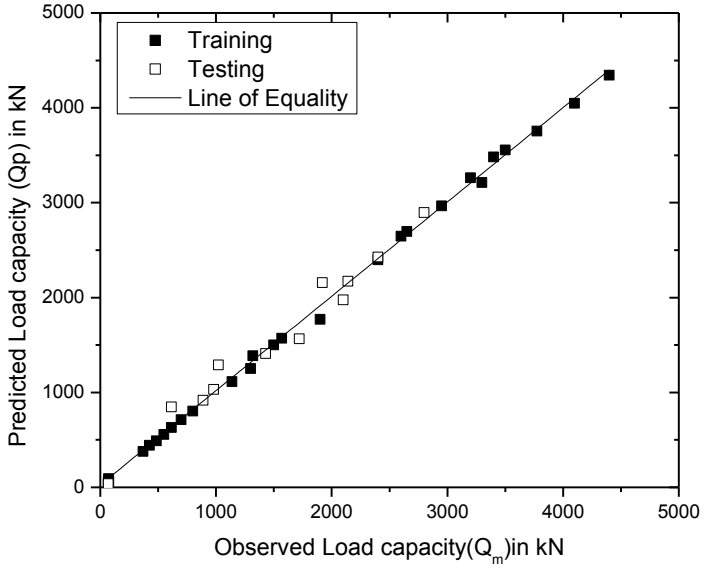

Figure.5.1. Comparison of predicted and measured bearing capacity by MARS for training and testing data in Static case

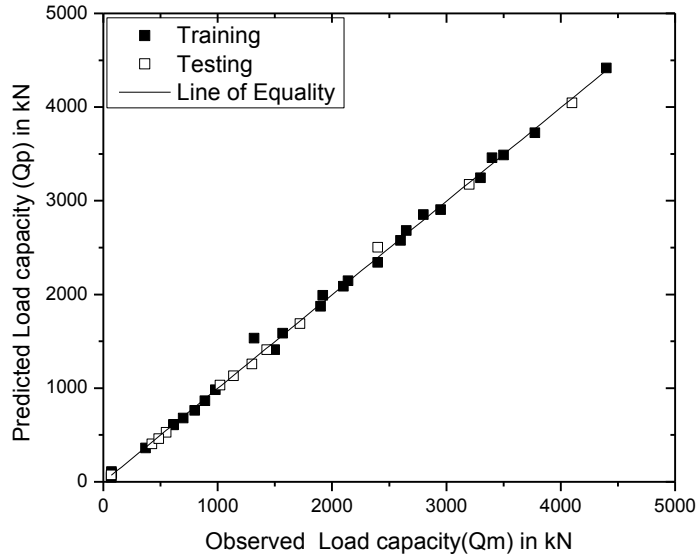

Figure.5.2. Comparison of predicted and measured bearing capacity by MGGP in Static case

Table.5.3 shows the statistical performance in terms of R, E, AAE, MAE and RMSE for the GP and MARS models for both training and testing data set.

Where,

R - Correlation coefficient

E - Coefficient of efficiency

AAE - Average absolute error

MAE - Maximum absolute error

RMSE - Root mean square error

The developed GP, MARS models shows good generalization in terms of close values of R and E for training and testing data. It can be seen that for both and training and testing data set, as per R and E values, MGGP is better than MARS values. Though, the AAE values for MARS is better than MGGP model, but MAE and RMSE values of MGGP is better than MARS model for the testing data. As per Das and Basudhar (2008), the efficiency of the model should be compared in terms of testing data than training data. Hence, in overall, based on different statistical performance criteria it can be seen that MGGP model is better than that of MARS model.

Table.5.3 Statistical performance of MGGP and MARS model for Static case

Model		Statistical performance				
		R	E	AAE	MAE	RMSE
MGGP	Training	0.99	0.99	36.675	90	54.56
	Testing	0.99	0.99	230	56.2	41.33
MARS	Training	0.99	0.99	33.39	129	45.80
	Testing	0.98	0.96	140.66	269	108.416

5.4 Prediction model for Dynamic case

In this present dynamic study the experimental data obtained through the laboratory investigation is considered to develop the empirical models. In total there are 400 numbers

of data points, out of which 286 data has taken for the training and remaining data taken for testing of the result. The input variable has taken as load carrying capacity of the unpaved road(Q), number of cycles (N) , thickness of the GSB (t) and corresponding settlement of geogrid reinforced unpaved road(S_e) is taken as output.. Similar to static load case, the data were normalized in the range 0 to 1 to avoid the dimensional effect of input parameters for MARS. In the GP modelling normalization or scaling of the data is not required.

Table.5.4 Training data for prediction of settlement in Dynamic case

Thickness (mm)	Number of cycle	Load (kN/m^2)	Settlement (Experiment) (mm)	Settlement (MARS)(mm)	Settlement (GP)(mm)
300	630	1942.70	35.10	34.92	34.89
200	1470	136.20	24.85	24.69	25.24
300	1740	2440.70	56.60	55.21	54.09
200	1230	135.00	22.95	22.80	22.75
250	1950	394.70	37.33	37.72	41.14
250	1260	396.70	31.90	30.80	31.48
250	930	1943.70	27.58	27.49	25.99
150	2580	1121.80	28.18	29.77	27.82
300	2850	2061.80	74.10	75.51	73.93
250	990	1944.70	27.95	28.09	26.83
300	1290	2438.50	49.30	46.98	46.16
200	450	1946.40	17.15	17.80	13.94
150	2280	1124.10	25.40	27.48	25.80
250	510	1944.10	23.53	23.28	20.11
300	750	1943.40	36.70	37.11	37.01
300	2250	2062.60	64.60	64.54	63.36
250	1200	396.40	31.23	30.20	30.64
200	180	1945.70	13.45	15.70	11.15
200	750	1946.50	19.53	20.13	17.05
250	1230	397.00	31.58	30.50	31.06
200	1740	136.30	26.45	26.61	28.04
200	2040	136.80	28.03	28.86	31.15
150	2670	1124.30	28.90	30.44	28.42
200	960	1948.20	20.75	21.76	19.23
150	2910	1118.00	30.80	32.31	30.04
200	1590	136.30	25.58	25.55	26.48
250	2610	2908.30	43.80	44.33	48.95
250	1470	400.80	33.90	32.90	34.42

250	1440	398.90	33.65	32.60	34.00
250	210	1941.90	18.35	20.27	15.92
200	2280	173.20	35.83	36.84	33.62
300	2790	2060.60	73.30	74.41	72.87
300	1410	2440.50	51.60	49.18	48.28
300	1980	2439.00	59.80	59.60	58.32
200	2010	136.80	27.90	28.65	30.83
150	930	1948.50	15.93	15.56	16.52
150	1020	1946.50	16.28	16.06	17.12
300	390	1943.60	30.90	30.53	30.66
250	1560	398.90	34.63	33.81	35.68
200	1410	137.30	24.40	24.49	24.62
250	1650	400.70	35.35	34.71	36.94
150	390	1946.70	12.75	12.59	12.88
300	510	1942.20	33.20	32.72	32.78
200	540	1944.70	17.98	18.50	14.88
150	2250	1123.00	25.10	27.26	25.60
300	210	1940.10	26.00	27.24	27.49
250	2940	2909.00	50.28	47.64	53.57
200	90	1942.10	10.98	11.64	10.22
150	2790	1117.90	29.90	31.39	29.23
250	1350	401.30	32.83	31.70	32.74
250	1890	396.70	36.95	37.11	40.30
250	660	1943.70	25.23	24.78	22.21
250	90	1939.10	14.10	15.78	14.24
300	1650	2442.30	55.30	53.57	52.51
250	2040	2909.30	38.10	38.62	40.98
300	2190	2064.40	63.40	63.44	62.30
300	810	1944.20	37.40	38.21	38.06
250	60	1938.30	12.30	12.18	13.82
250	720	1945.40	25.80	25.39	23.05
250	1500	399.20	34.15	33.21	34.84
300	930	1944.40	38.70	40.40	40.18
300	2730	2063.10	72.40	73.31	71.81
250	150	1941.60	16.55	19.67	15.08
250	1920	395.10	37.15	37.42	40.72
150	1170	2088.50	17.65	16.51	18.10
200	2460	172.00	38.90	38.65	35.48
300	600	1944.50	34.60	34.37	34.36
300	2490	2061.80	68.60	68.93	67.59
150	1500	2089.70	20.00	18.21	20.32
200	1110	136.20	21.80	22.17	21.51
300	1020	2436.70	42.40	42.05	41.41
300	2160	2062.20	62.80	62.89	61.77

200	1530	139.60	25.23	25.86	25.86
300	1620	2441.30	54.90	53.02	51.98
250	120	1940.80	15.43	19.37	14.66
150	1320	2088.10	18.85	17.29	19.11
300	180	1940.60	24.90	26.69	26.96
150	2010	2089.90	22.58	20.84	23.75
200	1050	135.20	21.08	21.60	20.89
250	2700	2908.20	44.55	45.23	50.21
150	150	1944.90	9.83	11.27	11.27
200	2310	169.40	36.40	37.15	33.93
200	1860	135.30	27.13	27.18	29.28
300	1110	2440.00	45.30	43.69	42.99
300	2940	2059.30	75.20	77.15	75.52
200	780	1947.50	19.73	20.36	17.36
200	2580	168.10	40.58	39.86	36.73
150	2850	1119.80	30.35	31.84	29.63
150	2760	1120.00	29.65	31.15	29.03
200	300	1946.70	15.43	16.63	12.39
250	2880	2910.30	49.55	47.04	52.73
150	1530	2088.20	20.18	18.37	20.52
250	1590	399.20	34.88	34.11	36.10
250	1620	400.80	35.10	34.41	36.52
250	1110	392.40	30.10	29.30	29.38
300	2610	2063.20	70.70	71.12	69.70
150	240	1945.90	11.18	11.76	11.87
250	2550	2909.00	43.15	43.73	48.11
250	2430	2908.80	42.08	42.53	46.43
150	2490	1121.50	27.40	29.09	27.21
250	1	1869.10	2.25	5.12	13.03
150	1230	2091.20	18.18	16.82	18.50
250	2250	2908.20	40.45	40.72	43.91
250	2520	2908.30	42.88	43.43	47.69
200	2550	170.50	40.18	39.55	36.42
150	2940	1121.30	31.03	32.51	30.24
150	810	1948.20	15.40	14.90	15.71
300	30	1930.40	13.80	14.81	24.33
200	2940	162.00	44.73	43.48	40.46
150	2970	1118.90	31.20	32.76	30.44
250	450	1944.70	22.75	22.68	19.27
300	570	1942.60	34.20	33.82	33.84
300	660	1943.70	35.50	35.47	35.42
200	2760	160.20	42.73	41.69	38.60
250	2130	2909.80	39.18	39.52	42.23
150	1	1921.50	2.68	-3.15	10.27

300	1320	2439.30	49.90	47.53	46.69
200	1500	137.50	25.00	25.18	25.55
300	450	1943.60	32.10	31.63	31.72
200	2430	171.80	38.48	38.35	35.17
300	240	1940.60	27.00	27.79	28.02
250	2640	2907.70	44.08	44.63	49.37
150	1350	2090.70	19.05	17.44	19.31
300	480	1942.60	32.70	32.17	32.25
250	630	1945.70	24.93	24.48	21.79
300	2640	2063.60	71.10	71.67	70.23
150	2820	1122.10	30.13	31.59	29.43
300	330	1944.50	29.50	29.43	29.61
300	2550	2060.90	69.60	70.02	68.64
200	2610	167.40	40.95	40.16	37.04
200	240	1945.40	14.53	16.17	11.77
300	2520	2060.30	69.10	69.47	68.12
250	540	1946.00	23.90	23.58	20.53
250	1830	397.70	36.60	36.51	39.46
150	2730	1118.20	29.40	30.94	28.83
300	2040	2062.10	60.20	60.70	59.66
250	750	1945.90	26.05	25.69	23.47
200	930	1948.70	20.58	21.53	18.92
150	1410	2090.50	19.43	17.74	19.71
250	1050	388.50	29.23	28.69	28.55
200	2160	172.30	32.53	35.64	32.37
300	1380	2439.00	51.10	48.63	47.75
150	480	1949.00	13.53	13.08	13.49
250	600	1944.20	24.60	24.18	21.37
300	1470	2440.80	52.60	50.28	49.33
200	1170	135.70	22.43	22.51	22.13
300	2100	2062.90	61.50	61.79	60.71
150	1590	2090.00	20.55	18.67	20.92
300	2370	2062.70	66.70	66.73	65.47
300	1950	2441.00	59.30	59.05	57.79
150	660	1947.20	14.63	14.08	14.70
150	2040	2091.80	22.68	20.98	23.95
300	270	1943.10	27.90	28.33	28.55
300	2430	2063.60	67.60	67.83	66.53
150	300	1947.50	11.93	12.09	12.28
150	1740	2087.40	21.30	19.46	21.93
300	420	1943.10	31.50	31.08	31.19
150	2100	1124.90	23.30	26.12	24.59
150	30	1940.10	6.38	0.32	10.46
300	990	1944.90	39.30	41.50	41.24

250	2370	2908.20	41.55	41.93	45.59
200	510	1946.40	17.73	18.27	14.57
300	2670	2061.90	71.60	72.22	70.76
300	1260	2438.80	48.80	46.44	45.63
300	300	1941.90	28.80	28.88	29.08
200	1080	134.70	21.48	21.73	21.20
250	2220	2909.60	40.13	40.42	43.49
150	690	1947.80	14.80	14.24	14.90
150	510	1949.60	13.70	13.25	13.69
300	2340	2062.10	66.20	66.18	64.94
150	1110	2091.30	17.08	16.20	17.69
300	2460	2060.40	68.10	68.38	67.06
200	2850	147.00	43.75	38.95	39.53
200	0	0.00	0.00	0.86	10.06
200	1980	135.30	27.75	28.00	30.52
150	1260	2089.40	18.43	16.98	18.70
200	2880	163.80	44.13	42.88	39.84
200	420	1947.70	16.85	17.57	13.63
200	600	1946.50	18.50	18.97	15.50
200	900	1947.80	20.43	21.29	18.61
200	810	1947.20	19.88	20.60	17.67
200	570	1947.20	18.25	18.73	15.19
300	2820	2061.40	73.70	74.96	73.40
200	2910	157.00	44.45	43.20	40.15
200	210	1942.90	14.00	15.94	11.46
250	2070	2910.30	38.48	38.92	41.39
150	270	1947.80	11.58	11.93	12.07
150	1380	2089.00	19.25	17.60	19.51
150	1920	2089.90	22.13	20.37	23.14
300	1200	2438.70	47.50	45.34	44.58
250	330	1946.20	20.90	21.48	17.59
300	1	1805.50	2.60	11.34	23.91
250	810	1945.50	26.58	26.29	24.31
150	960	1949.50	16.05	15.73	16.72
250	2790	2909.00	45.50	46.14	51.47
300	960	1943.60	39.00	40.95	40.71
200	1020	136.80	20.68	21.62	20.58
300	120	1938.60	22.00	25.59	25.91
300	1440	2441.10	52.10	49.73	48.81
200	480	1946.00	17.45	18.03	14.26
300	1800	2440.30	57.40	56.31	55.15
250	2970	2908.80	50.68	47.94	53.99
250	1800	397.90	36.43	36.21	39.04
150	2640	1119.20	28.68	30.25	28.22

300	1140	2438.40	46.10	44.24	43.52
200	2220	169.90	34.43	36.25	33.00
150	990	1948.30	16.18	15.89	16.92
150	2460	1123.30	27.10	28.85	27.01
300	1530	2439.30	53.60	51.37	50.39
250	960	1945.90	27.73	27.79	26.41
200	1800	135.20	26.78	26.74	28.66
250	2460	2906.80	42.30	42.83	46.85
250	420	1944.90	22.33	22.38	18.85
200	1320	137.30	23.70	23.85	23.68
150	2550	1121.00	27.93	29.55	27.62
200	1890	134.40	27.25	27.13	29.59
300	1830	2441.80	57.80	56.86	55.68
300	690	1944.20	35.90	36.01	35.95
200	630	1948.00	18.70	19.20	15.81
300	3000	2062.70	75.90	78.25	76.57
250	2190	2909.10	39.80	40.12	43.07
150	1830	2091.30	21.75	19.90	22.54
150	2340	1118.70	25.98	27.97	26.20
200	2700	166.90	42.10	41.06	37.97
200	2730	164.00	42.40	41.37	38.28
150	540	1945.40	13.95	13.42	13.89
150	750	1946.40	15.13	14.57	15.30
300	1050	2436.70	43.50	42.60	41.94
200	330	1945.90	15.80	16.87	12.70
200	1620	133.00	25.78	24.99	26.80
250	1140	394.70	30.48	29.60	29.80
250	870	1944.50	27.13	26.89	25.15
250	180	1941.90	17.53	19.97	15.50
150	870	1948.20	15.65	15.23	16.11
250	2670	2906.80	44.33	44.93	49.79
300	540	1942.70	33.70	33.27	33.31
250	1320	399.30	32.55	31.40	32.32
150	330	1944.20	12.20	12.26	12.48
200	390	1945.90	16.53	17.33	13.32
250	2910	2908.20	49.90	47.34	53.15
200	360	1946.00	16.15	17.10	13.01
200	30	1938.60	8.15	4.46	9.60
300	1080	2436.40	44.50	43.14	42.46
300	1860	2441.30	58.20	57.41	56.21
150	90	1945.00	8.50	7.51	10.86
250	840	1944.70	26.83	26.59	24.73
250	1410	397.50	33.38	32.30	33.58
150	2310	1121.50	25.70	27.73	26.00

150	1200	2090.00	17.90	16.66	18.30
150	840	1948.50	15.53	15.07	15.91
200	1290	136.00	23.48	23.39	23.37
200	2070	2433.80	29.90	29.19	30.53
200	270	1943.90	14.95	16.40	12.08
150	1770	2092.80	21.45	19.59	22.13
250	2730	2909.30	44.80	45.54	50.63
200	1650	134.00	25.98	25.43	27.11
300	1710	2440.80	56.20	54.66	53.56
150	1950	2092.50	22.33	20.52	23.35
150	1680	2091.80	21.00	19.13	21.53
200	1350	137.00	23.98	24.00	24.00
250	1770	399.50	36.23	35.91	38.61
250	2820	2908.70	46.05	46.44	51.89
200	1680	138.50	26.13	26.72	27.41
150	2880	1123.50	30.60	32.04	29.84
300	60	1935.30	17.30	18.40	24.85
150	2220	1124.80	24.73	27.03	25.39
250	360	1943.70	21.40	21.78	18.01
250	2100	2909.50	38.83	39.22	41.81
150	2130	1123.00	23.70	26.35	24.79
250	1860	397.40	36.83	36.81	39.88
150	2430	1121.30	26.88	28.64	26.81
200	2970	159.80	44.98	43.79	40.77
150	210	1945.00	10.80	11.60	11.67
300	2970	2059.90	75.50	77.70	76.05
250	1290	398.40	32.23	31.10	31.90
300	2280	2062.40	65.10	65.09	63.88
250	30	1934.70	9.75	8.59	13.40
200	2130	2440.00	32.08	29.60	31.15
300	360	1942.70	30.20	29.98	30.14
200	1830	137.50	26.93	27.56	28.97
300	1230	2442.10	48.20	45.89	45.10
150	2610	1124.60	28.43	29.98	28.02
250	1710	400.70	35.80	35.31	37.77
250	900	1944.50	27.35	27.19	25.57
200	2790	155.60	43.10	42.00	38.91
300	2910	2062.20	74.80	76.60	74.99

Table.5.5 Testing data for prediction of settlement for dynamic test

Thickness (mm)	Number of cycle	Load (kN/m^2)	Settlement (Experiment) (mm)	Settlement (MARS) (mm)	Settlement (GP) (mm)
150	570	1948.8	14.1	13.58	14.09
200	690	1945.2	19.125	19.67	16.43
150	1560	2091.2	20.325	18.51	20.72
200	1920	136	27.4	27.78	29.90
300	2700	2072.6	72	72.76	71.28
150	1890	2091.2	22.025	20.21	22.94
250	270	1943.1	19.75	20.87	16.75
200	1380	137.3	24.175	24.28	24.31
250	2340	2908.7	41.25	41.63	45.17
250	1740	400.2	36.025	35.61	38.19
300	2310	2063.4	65.6	65.63	64.41
300	2010	2443.5	60.2	60.15	58.85
300	1500	2440	53.1	50.82	49.86
200	990	1947.8	20.85	21.99	19.54
150	600	1947.7	14.275	13.75	14.29
150	2400	1123.3	26.575	28.4	26.61
250	0	0	0	5	14.07
200	1140	137.5	22.075	22.59	21.82
300	2880	2065.7	74.4	76.06	74.46
250	2280	2908.8	40.725	41.02	44.33
250	2160	2908	39.5	39.82	42.65
200	1	1905.3	3.35	0.98	9.31
150	630	1947.5	14.475	13.91	14.50
300	1890	2441.1	58.6	57.95	56.74
200	2340	168.4	36.975	37.46	34.24
150	1140	2089.2	17.35	16.36	17.90
200	2400	172.3	37.975	38.05	34.86
200	60	1940.8	9.8	8.05	9.91
200	2520	169.9	39.8	39.25	36.11
250	1530	399.5	34.375	33.51	35.26
200	870	1945.4	20.25	21.06	18.30
250	2850	2909	48.4	46.74	52.31
200	2100	2440.7	31.175	29.39	30.84
250	1380	399.5	33.125	32	33.16
200	2820	151.3	43.45	40.49	39.22
250	2760	2905.2	45.025	45.84	51.05
150	1440	2089.9	19.65	17.9	19.91
300	870	1942.9	38.1	39.31	39.12
150	360	1947.7	12.525	12.42	12.68
300	1350	2440.3	50.5	48.08	47.22

300	1560	2440.8	54	51.92	50.92
200	660	1947.3	18.925	19.43	16.12
200	1770	136.2	26.6	26.79	28.35
300	1590	2440	54.5	52.47	51.45
300	1680	2442.3	55.8	54.12	53.03
150	420	1947.8	13.05	12.75	13.08
200	2670	165.8	41.7	40.77	37.66
250	240	1945.5	19.05	20.57	16.33
250	1020	384.9	28.725	28.39	28.13
150	180	1946.2	10.35	11.43	11.47
300	2130	2062.4	62.2	62.34	61.24
200	1260	138	23.2	23.54	23.06
200	2640	169.2	41.35	40.46	37.35
300	840	1942.6	37.7	38.76	38.59
250	3000	2908.8	51.2	48.24	54.41
300	2070	2064.5	60.9	61.25	60.18
150	450	1945.5	13.275	12.92	13.29
150	1290	2089.5	18.625	17.13	18.90
250	1080	391.3	29.675	28.99	28.96
200	2490	168.4	39.325	38.96	35.80
200	150	1941.9	12.75	15.47	10.84
150	780	1946.8	15.275	14.74	15.51
300	1920	2441.6	59	58.5	57.26
250	1680	402.3	35.575	35.01	37.35
150	1710	2091	21.15	19.29	21.73
150	60	1941.6	7.625	3.91	10.66
200	1710	134.4	26.275	25.92	27.73
300	720	1943.7	36.3	36.56	36.48
300	2760	2064.2	72.9	73.86	72.34
200	720	1947	19.35	19.9	16.74
200	1440	136.5	24.625	24.54	24.93
300	2220	2062.6	64	63.99	62.83
150	3000	1123.3	31.425	32.95	30.64
150	1080	2092.8	16.775	16.04	17.49
150	1980	2086.6	22.45	20.7	23.55
150	2700	1123	29.125	30.68	28.62
250	390	1943.7	21.85	22.08	18.43
300	2580	2057.6	70.2	70.57	69.18
300	1770	2441	57	55.76	54.62
250	780	1943.9	26.35	25.99	23.89
250	2310	2911.1	41.025	41.33	44.75
150	2160	1118.9	24.075	26.6	24.99
200	3000	160.2	45.25	44.09	41.08
150	1050	2089	16.375	15.89	17.29

300	780	1942.7	37	37.66	37.54
200	3000	160.2	45.25	44.09	41.08
200	2370	170.5	37.45	37.75	34.55
250	690	1946.5	25.5	25.09	22.63
300	90	1938.3	19.9	22	25.38
300	900	1944.4	38.4	39.85	39.65
300	0	0	0	11.22	25.21
250	300	1945.2	20.325	21.18	17.17
200	1560	137.3	25.4	25.57	26.17
250	2580	2909	43.45	44.03	48.53
150	1860	2087.1	21.875	20.08	22.74
250	1170	393.3	30.875	29.9	30.22
250	2400	2908.5	41.8	42.23	46.01
200	1200	134.4	22.7	22.5	22.44
200	2190	170.4	33.6	35.95	32.69
200	2250	171.3	35.175	36.55	33.31
250	2490	2908.8	42.575	43.13	47.27
150	720	1947.8	14.95	14.41	15.10
200	1950	137.2	27.575	28.34	30.21
200	840	1947.3	20.075	20.83	17.98
150	2370	1125.3	26.3	28.16	26.40
150	2520	1122.1	27.65	29.32	27.41
150	900	1947.8	15.8	15.4	16.31
250	1980	394.7	37.475	38.02	41.56
250	2010	2906.7	37.675	38.32	40.56
150	1650	2090.8	20.825	18.98	21.33
250	570	1946	24.275	23.88	20.95
150	1620	2087.4	20.7	18.84	21.13
300	150	1940.1	23.5	26.14	26.44
250	480	1944.2	23.125	22.98	19.69
200	120	1943.2	11.95	15.24	10.53
300	2400	2064.2	67.1	67.28	66.00
150	1800	2090.7	21.6	19.75	22.34
150	1470	2088.9	19.825	18.06	20.12
300	1170	2439.2	46.8	44.79	44.05
150	120	1944.1	9.225	11.1	11.06
150	2070	1122.5	22.9	25.9	24.38
150	2190	1125.1	24.45	26.8	25.19

Table 5.4 shows the training database, based on which the prediction model using MARS and GP was developed. The developed MARS and GP models are validated using the testing database as shown in Table 5.5.

Prediction model as per MARS

In this section the prediction model as per MARS is presented and the GP model is presented in the next section.6 basis functions are used the develop the model in present study. The coefficients of different basis functions produced for the developed MARS mode, model equations can be written using the obtained coefficients and basis functions as presented in Equation 5.5 as follows

$$Y = 0.009 + 0.29x_1 + 3.54x_2 - 0.98x_3 - 53.34x_1x_2x_3 + 35.19x_2x_3 + 2.46x_1x_2 + 2.13x_1x_3 \quad (5.5)$$

Prediction model as per MGGP

In the present study each individual in the population consists of more than one gene and each gene is a traditional GP tree. Here, function set used include: +, ×, ÷, -, and exp. As discussed earlier in MGGP procedure first a number of potential models are evolved at random. Each model is trained and tested using the training and testing cases respectively. The fitness of each model is determined by minimizing RMSE between the predicted settlement (S_{e_p}) and actual settlement (S_{e_m}) value of the output variable as the objective function.

The best (S_{e_p}) model was obtained with population size of 1000 individuals and 100 generations with reproduction probability of 0.05, crossover probability of 0.85, mutation probability of 0.1 and with tournament selection. In this study optimum result was obtained with maximum number of genes as two and maximum depth of GP tree as four. The developed MGGP model can be described as above equation as shown in below equ(5.6).

$$Y = 24.64 - 0.001x_2 - 5.949\left(\frac{x_1x_2}{10^5}\right) - 0.0005x_3 - 0.1905\sin(\cos(x_1))\ (x_1 - 26.3) \quad (5.6)$$

These two Prediction model as shown in Equations 5.5 and 5.6 can be used in future for prediction of settlement in any prototype/full-scale Geogrid Reinforced Unpaved Road.

The variations of predicted and observed values of (S_{e_p}) for training and testing data as

per MARS and GP modelling are shown in Figure 5.3 and Figure 5.4, along with line of equality. It can be seen, comparison to MARS modelling, there is less number scattering in data as compared to MGGP. These two equations(5.5) and (5.6) can be used in future for prediction of settlement in any prototype/full-scale Geogrid Reinforced Unpaved Road.

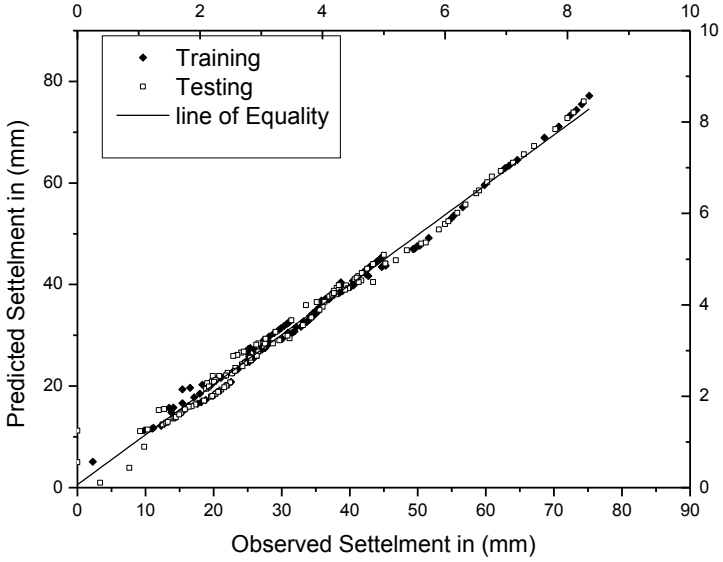

Figure.5.3. Comparison of predicted and measured bearing capacity by MARS for training data in Dynamic case

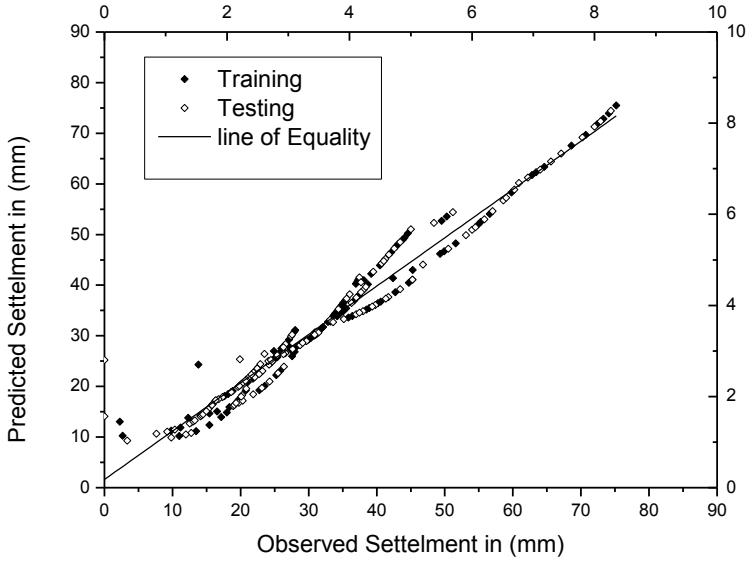

Figure.5.4. Comparison of predicted and measured bearing capacity by GP for testing data in Dynamic case

Table.5.4 shows the statistical performance in terms of R, E, AAE, MAE and RMSE for the GP and MARS models for both training and testing data set.

The developed GP and MARS models show good generalization in terms of close values of R and E for training and testing data. It can be seen that for both and training and testing data set, as per R and E values, MARS is better than MGGP values. It can be seen that for both and training and testing data set, as per R and E values, MARS is better than MGGP values. Similarly, the AAE, MAE and RMSE values for MARS is better than MGGP model for both training and testing data. Hence, in overall, based on different statistical performance criteria it can be seen that MARS model is better than that MGGP of model.

Table.5.6 Statistical performance of MGGP and MARS model for Dynamic case

Model		Statistical performance				
		R	E	AAE	MAE	RMSE
GP	Training	0.96	0.99	1.92	10.72	2.82
	Testing	0.95	0.98	2.29	25	3.50
MARS	Training	0.99	0.99	1.06	8.74	2
	Testing	0.99	0.99	1.19	11.21	1.83

5.5 Sensitivity Analysis

The sensitivity analysis is an important aspect of a developed model to find out important input parameters. In the present study sensitivity analysis was made by GP models. By the developed GP model sensitivity analysis was made according to Gandomi et al. (2013). As per Gandomi et al. (2013) the sensitivity (S_i) of each parameter, is expressed by the following equation

$$S_i = \frac{N_i}{\sum_{j=1}^{n} N_j} x100 \quad (5.5)$$

$$N_i = f_{max}(x_i) - f_{min}(x_i) \quad (5.6)$$

Where $f_{max}(x_i)$ and $f_{min}(x_i)$ are the maximum and minimum of the predicted output over the i^{th} input domain, where the other variables are equal to their mean values and n is the number of variables. In the present study n=4. It can be seen that for the static load case, the sensitivity analysis of both MGGP and MARS shows settlement as the most important input parameter. The second important input parameters varies for MGGP and MARS, as both thickness and elastic modulus of GSB layer are important with elastic modulus of sand (subgarde) is least important parameter.

In the case of dynamic case, load is the most important parameter as per both MGGP and MARS. But, second important input parameter is thickness of the GSB and number of cycles, as per MGGP and MARS, respectively. As MARS prediction model was found to better than MGGP, in the present study, the number of cycle is considered as more important input than the thickness of GSB.

Table.5.7 Sensitivity analysis using GP and MARS for Static case

Parameters	Sensitivity Analysis in GP (%)	Ranking (GP model)	Sensitivity Analysis in MARS (%)	Ranking (MARS model)
Thickness of GSB (mm)	24	2	12.8	3
Settlement (mm)	61	1	46	1
Elastic Modulus Of GSB (MPa)	12	3	32	2
Elastic Modulus Of Sand (MPa)	3	4	8.9	4

Table.5.8 Sensitivity analysis using GP and MARS for Dynamic case

Parameters	Sensitivity Analysis in GP (%)	Ranking (GP model)	Sensitivity Analysis in MARS (%)	Ranking (MARS model)
Thickness of GSB (mm)	35	2	22	3
Load (Kg)	47	1	46	1
Number of cycles(N)	18	3	32	2

5.6 Result and Analysis

In this chapter, different models equations were presented for static and dynamic cases using both MGGP and MARS modelling. Based on different statistical performance criteria like R, E, AAE, MAE, RMSE, it was found that for the static load case, though both the model equations as per MGGP and MARS efficient, but MGGP was found to be more effective in comparison to MARS as followed in static case and MARS was found more effective in comparison to GP in dynamic case. Based on the sensitivity analysis in the Static case the settlement of the pavement has been found more important factor as followed by the thickness of GSB, Elastic modulus of subgrade and subbase in Static case and also in the case of dynamic, it has been found more important factor as followed by the settlement of the reinforced unpaved road, number of cycles and thickness of the GSB.

CHAPTER 6
GENERAL OBSERVATIONS, CONCLUSIONS, AND SCOPE OF FUTURE STUDIES

6.1 Summary

In the present study an attempt has been to analyze the geosynthetic reinforced unpaved roads. The state of the art of the geosythetic reinforced unpaved roads indicate, very limited experimental and numerical studies have been done in this regard. In the present study the experimental work consist of a laboratory investigation of the bearing capacity and settlement analysis of a model footing resting of layers of subabse and subgrade without reinforcement and with reinforcement at the interface of the subbase and subgrade. Both static and dynamic loads have been considered. The static load investigations have been validated using two commercial softwares, Plaxis^{2D} and FLAC^{2D}, which are based on FEM and FDM, respectively. Based on the database developed as per numerical analysis, empirical models are presented using two recently developed artificial intelligence techniques, MGGP and MARS. The dynamic test investigation was validated using a available numerical method and prediction models are proposed using MGGP and MARS based on the present experimental database.

6.2 Conclusions

Based on the above study the following conclusions can be made

1. It was observed that in case of static load, there is reduction of settlement upto 40% with addition of the reinforcement at the interface of subgrade and subbase. It was also observed that percentage of settlement reduction varied from 7.14% to 41.66% with increase in the depth of granular subbase from 150 to 300mm, showing the importance of subbase layer.

2. But in case of dynamic case settlement increased with increase in depth of granular sub base layer and decreased with provision of reinforcement irrespective of the number of cycles. The increase in settlement with increase in subbase layer may be due to the fact that the vertical load may transfer to the granular subbase at the immediate application of load and gradually it transfers into the subgrade.

3. It was observed that the settlement of model footing resting of reduced by 40 to 60% shown that by using geogrid reinforcement the settlement has reduced 40-60% as well as increase the bearing capacity with both Static and Dynamic case. The stress strain behaviour of geogrid reinforcement during Static loading has observed.

4. Based on the numerical validation of the experimental results as per FEM and FDM method it was observed that for static load case, it was observed that for unreinforced case there is wide variation in $FLAC^{2D}$ (8.6 to 35%) with that of experimental results in comparison to $Plaxis^{2D}$ result (25-30%). Whereas, for the reinforced case less variation was observed with $FLAC^{2D}$ (7-20%) than that of $Plaxis^{2D}$ (7-30%). For the dynamic load case reverse trends were observed between present experimental results and the existing empirical method.

5. For the static load case prediction models are presented for the bearing capacity of footing with thickness of the granular subbase, settlement of the circular footing, elastic modulus of base course, elastic modulus of subgrade as the inputs, using MGGP and MARS**.** Both MGGP and MARS models are efficient with correlation coefficient (R) value as 0.99 and 0.98, respectively. Based on different statistical parameters like coefficient of efficiency, MAE, AAE and RMSE, it was observed that MGGP model is more efficient than MARS model.

6. Sensitivity analysis of the model equation shows that the settlement of the pavement has been found more important factor followed by the thickness of GSB, elastic modulus of subgrade and subbase.

7. Similarly for the dynamic load case, model equations are presented for settlement of the footing using thickness of the GSB, number of cycle and load as the inputs. Based on statistical performance criteria R, E, AAE, MAE and RMSE, MARS model was found to more efficient than MGGP model.
8. The sensitivity analysis of the model equations shows that load is the most important factor as followed by the number of cycles and thickness of the GSB.

6.3 Scope for future study

Scope of application of geosynthetic to the unpaved road in geotechnical engineering problems is very promising. Some of the following problems are recognized for further studies.

i. Model studies using geocell along with geogrid and with saturated condition.
ii. Use of actual model parameters instead of correlated model parameters for the FEM and FDM validation of the laboratory findings.
iii. Reliability analysis of the geosynthetic/ geogrid reinforced unpaved roads using artificial intelligence techniques GP and MARS.

REFERENCES

Adel A. Al-Azzawi. (2012). "Finite element analysis of flexible pavements strengthed with geogrid". *ARPN Journal of Engineering and Applied Sciences,* Volume-7, 1295-1299.

Alavi, A. H., Aminian, P., Gandomi, A. H., and Esmaeili, M. A., (2011). "Genetic-based modeling of uplift capacity of suction caissons". *Expert Systems with Applications,* 38, 12608- 12618.

Alavi, A. H., and Gandomi, A. H., (2012). "Energy-based numerical models for assessment of soil liquefaction". *Geoscience Frontiers,* 3(4), 541-555.

Al-Qadi I., Dessouky S., Kwon J., and Tutumluer E., (2008). "Geogrid in flexible pavements: Validated mechanism." *Transportation Research Record 2045, Transportation Research Board,* Washington, DC, 102–109.

Babu Sivakumar, G.L., (2006). "An Introduction to soil reinforcement and geosynthetics". University press (I) Pvt ltd, India.

Benjamin, C.V.S., Bueno, B., and Zornberg, J.G., (2007). "Field monitoring evaluation of geotextile-reinforced soil retaining walls". *Geosynthetics International Journal,* Vol. 14, No. 1.

Benmebarek Naima., Benmebarek Sadok., and Belounar Lamine., (2013). "Performance improvement of road embankment on Algeria Sabkha soils by geosynthetics". *The Online Journal of Science and Technology,* Volume-3,101-108

Bueno, B.S., Costanzia, M.A., and Zornberg, J.G.. (2005). "Conventional and accelerated creep tests on nonwoven needle-punched geotextiles". *Geosynthetics International,* Vol. 12, No. 6, 276-287.

Burt G. Look.(2007) “Handbook of geotechnical investigation and design tables’’ *Taylor & Francis Group*, London, UK

Das, B.M., (1990). Earth Anchors. Elsevier,Netherland

Das, B.M., and Omar, M.T., (1994). “The effects of foundation width on model tests for the bearing capacity of sand with geogrid reinforcement”. *Geotechnical and Geological Engineering*, Vol. 12, 133–141.

Shin, E.C., Kim, D.H., and Das, B.M., 2002. “Geogrid reinforced rail road bed settlement due to cyclic load”. *Geotechnical and Geological Engineering*, Vol. 20, No. 3, 261-271.

Das, B.M. and Shin, E.C., (1994). “Strip Foundation on Geogrid - Reinforced Clay: Behavior Under Cyclic Loadings”. *Geotextiles and Geomembranes*, Vol. 13, 657-667.

Das, S.K., and Basudhar, P.K., (2006). “Undrained lateral load capacity of piles in clay using artificial neural network”. *Computational Geotechnics*, 33(8):454–459.

Das, S. K., and Samuai, P., (2008). “Prediction of liquefaction potential based on CPT data: A relevance vector machine approach”. *12th International Conference of International Association for Computer Methods and Advances in Geomechanics (IACMAG)*, Goa, India.

Das, S. K., and Muduli, P. K., (2011)., “Evaluation of liquefaction potential of soil using extreme learning machine”. *13th International conference of the International Association for Computer Methods and Advances in Geomechanics*, Melbourne, Austrailia, Khalili, N. and Oeser, M., eds.,1, 548-552.

Das, S.K., Biswal, R.K., Sivakugan, N., and Das, B., (2011). "Classification of slopes and prediction of factor of safety using differential evolution neural networks". *Environ Earth Science,* 64:201–210.

DeMerchant, M.R., Valsangkar, A.J., and Schriver, A.B., (2002). "Plate load tests on geogrid-reinforced expanded shale lightweight aggregate". *Geotextiles and Geomembranes,* 20(2002), 173 -190.

Giroud, J.P., and Noiray, L., (1981). "Geotextile reinforced unpaved road design". *Journal of the Geotechnical Division ASCE,* Volume.107, September 1981, 1233-1254.

Giroud, J.P., Bonaparte, R., and Holtz, R.D., (1985). "Soil reinforcement Design using Geotextile and Geogrid". ASTM symposium, *Geotextile testing and the Design engineer,* 69-116.

Giroud, J.P., and Jie Han., (2004). "Design method for geogrid reinforced unpaved roads. i. Development of Design Method". *Journal Geotechnical Geo environmental Engineering*. 775-786.

Giroud, J.P., and Jie Han. (2004). "Design method for geogrid reinforced unpaved roads. ii. Calibration and Application". *Journal Geotechnical Geo environmental Engineering*. 787-797.

Gu Jie., (2011). "Computational Modeling of Geogrid Reinforced Soil Foundation and Geogrid Reinforced Base in Flexible Pavement". *Ph.D. dissertation*. Louisiana State Univ., Baton Rouge, LA.

Henry Karen S.,Clapp Joshua.,Davids William., Humphrey Dana.,Barna Lynette., "Structural Improvements of Flexible Pavements Using Geosynthetics for Base Course

Reinforcement". ERDC/CRREL T R-09-11. Engineer Research and Development Center, Cold Region Research and Engineering Laboratory, Hanover, NH, USA.

Henry, K., Clapp, J., Davids, W., and Barna, L., (2011). " Back–calculated pavement layer modulus values of Geogrid reinforced test sections". Geo-Frontiers, 2011, 4673-4682.

Huang, C.C., and Menq, F.Y., (1997). "Deep footing and wide-slab effects on reinforced sandy ground". *Journal of Geotechnical and Geoenvironmental Engineering*, ASCE 123 (1), 30–36.

Jersey Sarah, R., and Tingle Jeb, S., 2009. "Cyclic plate testing of Geogrid-reinforced highway pavements Geotechnical and structures". Laboratory U.S. Army Engineer Research and Development Center.

Joanjun Leng., and Mohammed A Gabr., (2003). "Numerical analysis of stress deformation response in reinforced unpaved road sections". *Transpiration Research Board*, 1-26.

Khing, K.H., Das, B. M., Puri, V.K., Cook, E.E., and Yen, S.C., (1993). "The bearing capacity of a strip foundation on geogrid reinforced sand". *Geotextiles and Geomembranes*, Vol. 12, 351-361.

Kief Ofer., and Rajgopal, K., (2008). "Three Dimensional Cellular Confinement System Contributions to Structural Pavement Reinforcement". *Geosynthetics India seminar 2008*, 1-12.

Latha Madhavi, G., and Rajagopal K., (2007). "Parametric finite element analysis of geocell supported embankments". *Canadian Geotechnical Journal* (2007), Volume 44, 917-927.

Latha Madhavi, G., (2011). “Design of geocell reinforcement for supporting embankments on soft ground”. *Geomechanics and Engineering*, Vol. 3, No. 2 (2011), 117-130.

Liu Chia-Nan., Yang Kuo-Hsin., and Nguyen Duc Minh., (2014). “Behavior of geogrid reinforced sand and effect of reinforcement anchorage in large scale plane strain compression”. *Geotextiles and Geomembranes*, 42(2014), 479 - 493.

Mehdipour Iman., Ghazavi. Mahmoud., and Moayed Ziaie Reza., (2013).” Numerical study on stability analysis of geocell reinforced slopes by considering the bending effect”. *Geotextiles and Geomembranes*, 37(2013), 23-34.

Moghaddas Tafreshi, S.N., and Khalaj, O., 2008. “Laboratory tests of small-diameter HDPE pipes buried in reinforced sand under repeated load”. *Geotextiles and Geomembranes*, Vol. 26, No. 8,145-163.

Moghaddas Tafreshi, S.N., Tavakoli Mehrjardi Gh., and Ahamadi, M., (2011). “Experimental and numerical investigation on circular footing subjected to incremental cyclic loads”. *International Journal of Civil Engineering*, Volume 9, 265-274.

Nazzal Munir, D., Abu-Farsakh Murad, Y., and Mohammad Louay, N., (2010). “Implementation of a Critical State Two-Surface Model to evaluate the response of Geosynthetic reinforced pavement*”. International Journal of Geomechanics*, Vol. 10, 202-212.

Omar, M.T., Das, B.M., Puri, V.K., and Yen, S.C., 1993. “Ultimate bearing capacity of shallow foundations on sand with geogrid reinforcement”. *Canadian Geotechnical Journal*, Vol. 30, 545-549.

Palmeira Marques Ennio., (2009). "Soil–geosynthetic interaction: Modelling and analysis". *Geotextiles and Geomembranes,* 27(2009), 368-390.

Patra, C.R., Das, B.M., and Atalar, C., (2005). "Bearing capacity of embedded strip foundation on geogrid-reinforced sand". *Geotextiles and Geomembranes,* 23(2005), 454 - 462.

Perkins, S.W., (1999). "Mechanical response of Geosynthetic reinforced flexible pavement". *Geosynthetic International,* Vol.6, 347-382.

Perkins, S.W., (2001). "Mechanistic empirical modelling and design model development of geosynthetics reinforced flexible pavements". FHWA/MT-01- 002/99160-1A, U.S. Department of Transportation, Federal Highway Administration, Washington, DC.

Rajagopal, K., Veeragavan A., and Chandramouli S., (2012). "Studies on geocell reinforced road pavement structures". *5th Asian Regional Conference on Geosynthetics,* 497-502.

Raymond, G.P., and Komos F.E., (1978). "Repeated load testing on a model plane strain footing", *Canadian Geotechnical Journal,* Vol. 15, No. 2, 190-201.

Sah, N.K., Sheorey, P.R., and Upadhyama, L.W., (1994). "Maximum likelihood estimation of slope stability". *International Journal of Rock Mechanics and Mining Science & Geomechanics Abstracts,* 31:47–53.

Samui, P., Das, S.K., and Kim, D., (2011). "Uplift capacity of suction caisson in clay using multivariate adaptive regression spline". *Ocean Engineering,* 38(17–18), 2123-2127.

Shahin, M.A., Maier, H.R., and Jaksa, M.B., (2002). "Predicting settlement of shallow foundations using neural network". *Journal of Geotechnical. and Geoenvironmental. Engineering .,* ASCE, 128(9), 785- 793.

Shin EC., Das BM., Puri VK., Yen SC., Cook EE., (1993) "Bearing capacity of strip foundation on geogrid reinforced clay". Geotech Test J 16(4):534–541.

B.M Das and Shin E(1994) ., "Strip foundation on geogrid-reinforced clay behavior under cyclic loading" *Geotextiles and Geomembranes* Volume 13, Issue 10, 1994, 657-667

Shin, E.C., and Das, B.M., (2000). "Experimental study of bearing capacity of a strip foundation on geogrid reinforced sand". *Geosynthetics International,* Vol. 7(1), 59-71.

Yang, C. X., Tham, L. G., Feng, X. T., Wang, Y. J., and Lee, P. K., (2004). "Two stepped evolutionary algorithm and its application to stability analysis of slopes". Journal of Computing in Civil Engineering., ASCE, 18(2), 145-153.

Yang Xiaoming., Han Jie., Pokharel, K. Sanat., Manandhar Chandra., Parsons, L. Robert., Leshchinsky Dov., and Izhar Halahmi., (2013). "Accelerated pavement testing of unpaved roads with geocell reinforced sand bases". Geotextiles and Geomembranes, 32(2012), 95-103.

Zoenberg, J.G., (2012). "Geosynthetic reinforced pavement system". *5th European Geosynthetic Congress. Valencia,* (2012). 49-61.